Bayer, SA and J Altman (1991) NEOCORTICAL DEVELOPMENT Raven Press.

CHAPTER 10

Experimental Studies of Neocortical Development Using x-Irradiation

Exposure of an embryonic, fetal, or infant rat to ionizing radiation has a devastating effect on the developing central nervous system. Irradiation with a single dose of 150–200 R x-ray, for example, kills a high proportion of the stem cells of neurons and migrating young neurons, although it spares most of the mature neurons (Hicks and D'Amato, 1961, 1966; Altman et al., 1967, 1968). Within the embryonic nervous system there are regional differences in vulnerability and, as we shall show in this chapter, the cerebral cortex is one of its most vulnerable components. The technique of x-irradiation is, therefore, well-suited to determine which cell populations of the developing cortex are vulnerable and the critical periods of their vulnerability.

There are two experimental designs for studies of nervous system development with x-irradiation. The first is the acute paradigm in which the embryo is killed 6 hours after a single exposure to low-level x-ray. Pyknotic debris, the darkly staining remains of cellular breakdown (Fig. 10–1), is still present in the brain, usually in the same locations that the cells had occupied before they died (Fig. 10–1). The second is the longitudinal paradigm. Embryonic, fetal, or infant animals are irradiated when a particular neuronal population is known to be vulnerable. The animals are allowed to survive until the brain has matured and the effects of irradiation on brain structure and function are then assessed. The longitudinal studies also reveal the regenerative capacity of the decimated tissue. We have used the longitudinal paradigm in several brain regions, such as the cerebellum (Altman, 1982) and the hippocampus (Bayer and Altman, 1974, 1975a, 1975b). The experimental results described in this chapter are limited to the acute paradigm since we have not used the longitudinal approach in the developing cortex.

The details of the animal care procedures, the type of x-ray used, and the exposure levels are presented in detail in Appendix 6. In brief, timed pregnant Wistar rats received whole-body exposure to 200 R x-ray from a GE 300 Maxitron unit, and their embryos were removed by Cesarian section 6 hours later. During the early stages of its development, exposure of the brain to 200 R x-ray results in the collapse of a dorsal pallial

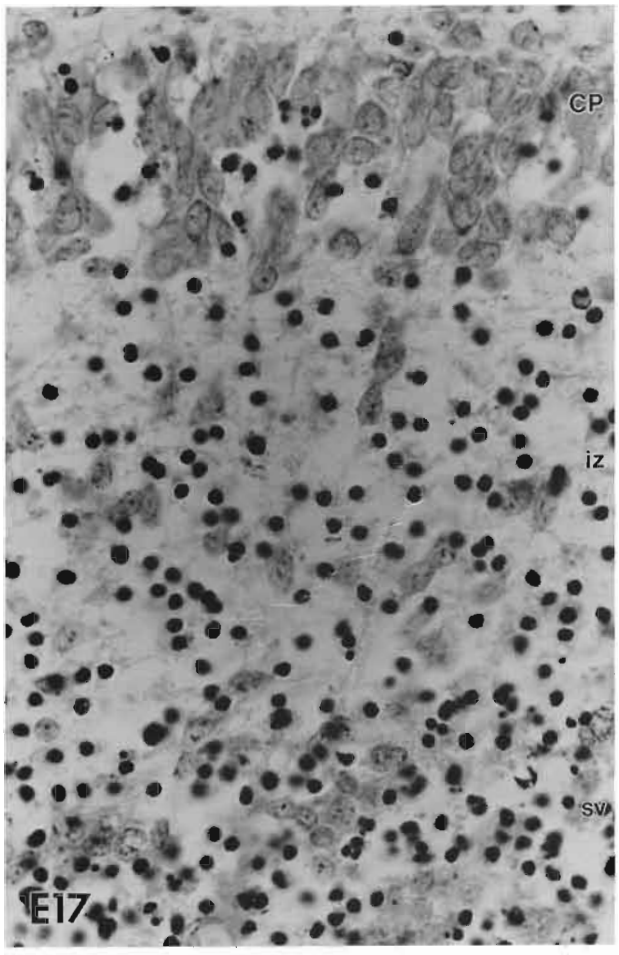

FIG. 10–1. A portion of the neocortex from an E17 rat that was exposed to 200 R x-ray *in utero* and was killed 6 hours after irradiation. The round opaque bodies are the pyknotic debris of the cells killed by x-ray. While many neurons in the cortical plate (CP) survive, most of the cells in the intermediate zone (iz) and subventricular zone (sv) have been killed. (3 μm methacrylate section, toluidine blue stain.)

area, the presumptive cortical primordium, in contrast to adjacent telencephalic regions that do not collapse. In Section 10.1, x-irradiation is used as a marker to delineate the boundaries of the presumptive cortical primordium before it becomes morphologically distinguishable from other components of the telencephalon. In Section 10.2, the response of the cortical neuroepithelium to x-irradiation on specific embryonic days is linked to the changing patterns of cell labeling seen with [^{3}H]thymidine autoradiography. First, we show that the total neuroepithelial collapse changes into a partial, or patchy, collapse as cortical development progresses, and we relate that change to the compartmentation of labeled and unlabeled cells in the neuroepithelium after [^{3}H]thymidine injections. In section 10.3, we correlate the increasing radioresistance of the neuroepithelium (more cells survive at later ages) to the shift from the early to the late labeling patterns after [^{3}H]thymidine injections (Chapter 4). In Section 10.4, we describe the differences in the vulnerability of various cellular components of the developing cortex after they have left the neuroepithelium. A qualitative analysis of these differences in the subventricular and intermediate zones in the lateral cortical stream and in different areas of the cortical plate provides some clues about age-dependent changes in neuronal vulnerability. In Section 10.5, we quantify the changes in radiosensitivity throughout the various layers of the dorsomedial cortex from E13 to E22 and relate those changes to many of the qualitative observations reported in Sections 10.1 and 10.2. Finally, in Section 10.6, we try to relate the results obtained with x-irradiation in rats to clinical studies of malformations of the human cerebral cortex during embryonic development.

10.1 THE PHENOMENON OF NEUROEPITHELIAL COLLAPSE AND THE DELINEATION OF THE CORTICAL PRIMORDIUM

Day E13

Figure 10–2A illustrates a sagittal section of the brain of an E13 rat that received a single dose of 200 R x-ray and was killed 6 hours later. At this low magnification, the pyknotic cells that abound throughout the neuroepithelium from the rhombencephalic vesicle (RC) caudally to the telencephalic vesicle (TC) rostrally are difficult to see. But what is obvious is the shedding of pyknotic debris into the lateral ventricle in the dorsal telencephalon (*area between the two arrows*). This is the phenomenon of neuroepithelial collapse. Our interpretation is that the x-irradiation kills most of the periventricular cells in this area so that the ventricular wall no longer remains intact, and pyknotic material spills into the ventricular lumen. We identify the dorsal collapsing telencephalic region as the presumptive neocortical neuroepithelium (cc). The location of the presumptive neocortical neuroepithelium in the coronal plane is shown in a similarly treated E13 rat in Fig. 10–2B (cc *between arrows*). In Fig. 10–2A, there is no neuroepithelial collapse in the presumptive hippocampus (hi) or in the presumptive basal telencephalon (bt). Except for a limited region of the mammillary recess (mr), there is no neuroepithelial collapse in any other brain region. Within the presumptive cortical neuroepithelium, the collapse is much more pronounced posteriorly than anteriorly at this early stage of development. If it were not for their different response to radiation, the noncollapsing area designated as the presumptive basal telencephalon (bt) anteriorly

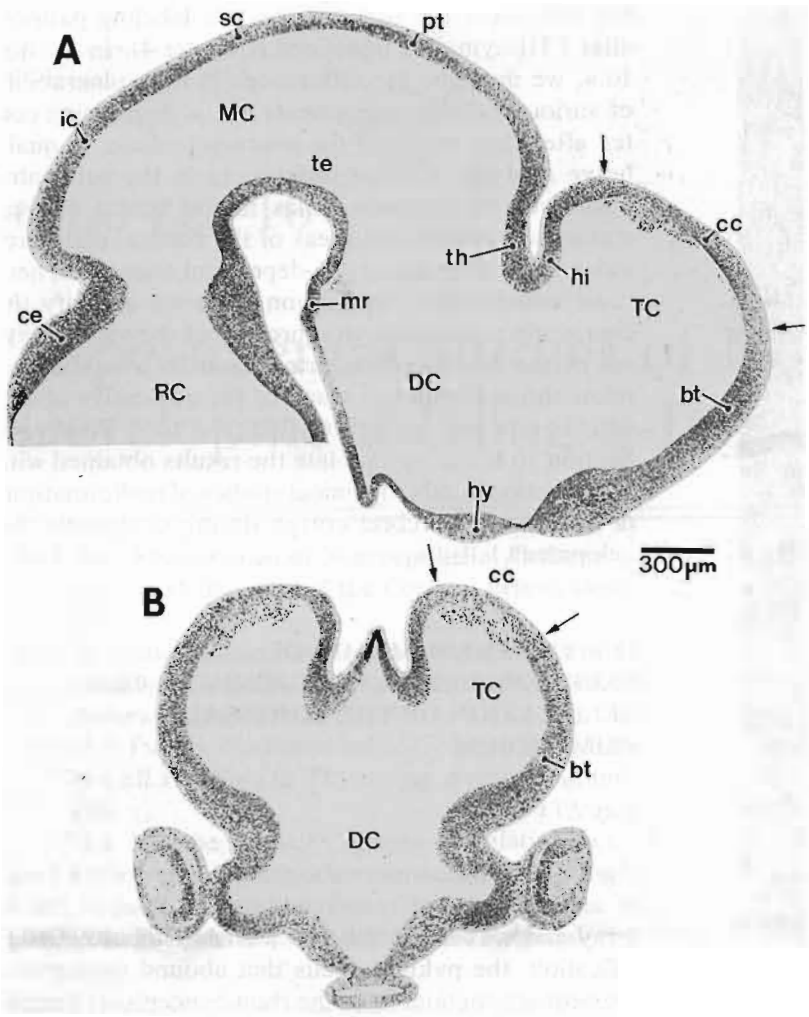

Note that Figure 10-2 shows the extent of the Lhx7-expressing neuroepithelium in the telencephalon on E13. [See the discussion of the new literature in Chapter 4.] The cortical phenotype is restricted to that part of the neuroepithelium that spills pyknotic debris into the lateral ventricles on E13, E14 (Figure 10-3), and E15 (Figure 10-4).

FIG. 10–2. (A) Sagittal section of the brain from an E13 rat that received a single dose of 200 R x-ray and was killed 6 hours afterward. The collapsing region in the dorsal telencephalon is the presumptive cerebral cortex (cc between arrows). **(B)** Coronal section at the level of the eye primordium from another, similarly treated E13 rat. The collapsing region between the two arrows is presumably the cortical neuroepithelium (cc). (3 μm methacrylate sections, toluidine blue stain.)

(Fig. 10–2A) and laterally (Fig. 10–2B) could not be distinguished from the presumptive cerebral cortex dorsally.

Day E14

Neuroepithelial collapse is more pronounced and more extensive following x-irradiation of E14 rats, but it is still limited to the dorsomedial and dorsal aspect of the telencephalon. In the sagittal section (Fig. 10–3A) collapse extends through most of the dorsal telencephalon (*area between two arrows*) and only a small band of superficial cells in the roof of the cortical primordium (the cells of the primordial plexiform layer) remain in place. There is some neuroepithelial collapse in the center of the septal primordium (se). In the coronal section (Fig. 10–3B), neuroepithelial collapse is limited to the dorsal and medial telencephalon. The spared lateral telencephalon, designated as a component of the basal telencephalon (bt), has become thicker than the presumptive cerebral cortex (note the increasing thickness of the telencephalic roof plate from dorsal to lateral).

Day E15

Cortical neuroepithelial collapse is most striking on this day in the sagittal plane (Fig. 10–4A). Except for a thin band of superficial cells, all the cells are killed in the dorsomedial sector of the cortex, and the edge of the ventricle is no longer visible. As on the previous day, the septal primordium (se) also shows partial collapse but the hippocampal (hi) and basal telencephalic (bt) primordia are spared. Examination of a horizontal section through the lateral cortex from another E15 rat (Fig. 10–4B) indicates that less pyknotic debris is shed into the ventricle posteriorly than anteriorly. The reduced neuroepithelial collapse is particularly pronounced adjacent to the noncollapsing hippocampal neuroepithelium (hi).

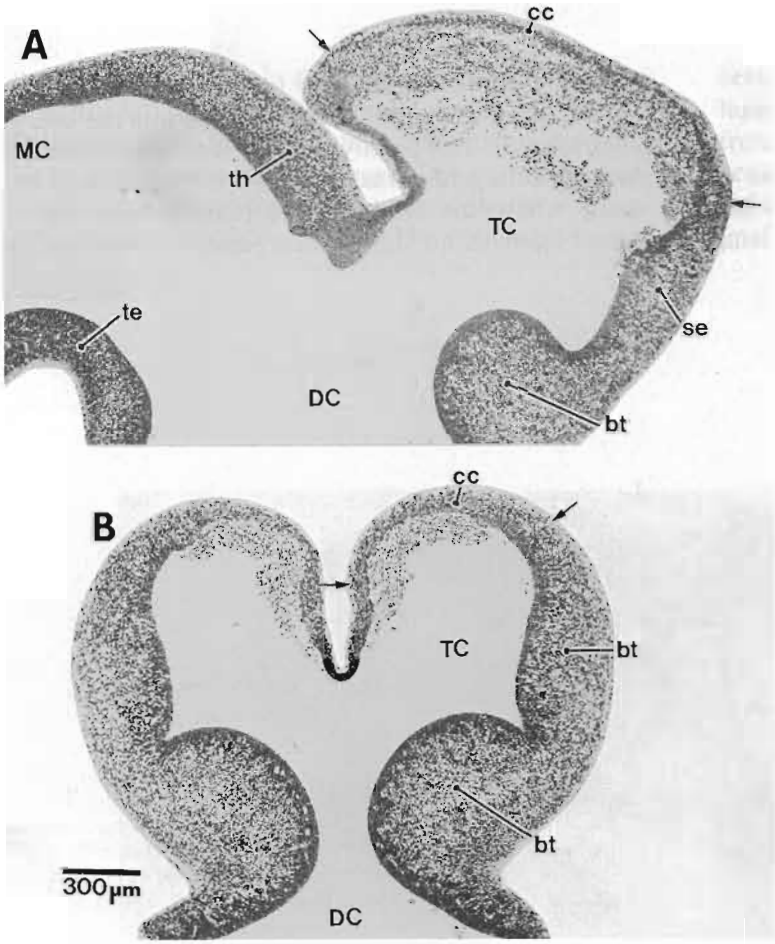

The cortical neuroepithelium has greatly expanded between E13 (Figure 10-3) and E14, as delineated by that part of the neuroepithelium that spills pyknotic debris into the lateral ventricle. This is the Lhx2-expressing neuroepithelium. Note that the "se" label is probably incorrect; that area may be the orbital area of the cortex.

FIG. 10–3. (A) Sagittal section of the forebrain from an E14 rat that received 200 R x-ray and was killed 6 hours later. The collapsing neuroepithelium between the arrows is identified as the primordium of the cerebral cortex. **(B)** Coronal section from a similarly treated E14 rat. (3 µm methacrylate sections, toluidine blue stain.)

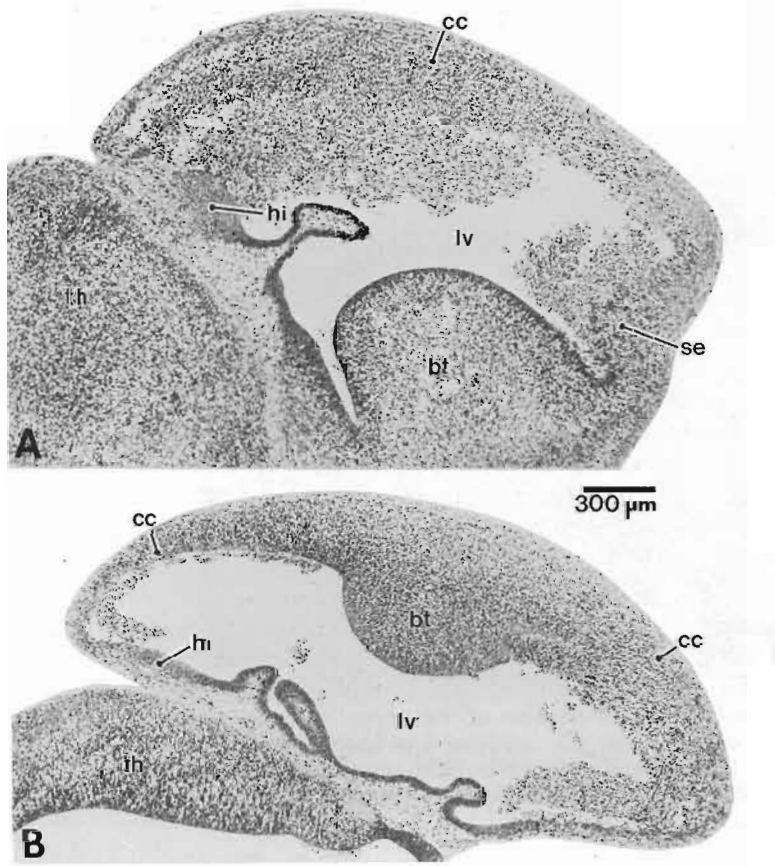

The Lhx2-expressing cortical neuroepithelium reaches its greatest extent on E15, as delineated by that part of the neuroepithelium that spills pyknotic debris into the lateral ventricle. Note that the "se" label is definitely incorrect here; that area is more clearly the orbital area of the cortex.

FIG. 10–4. (A) Sagittal section of the forebrain from an E15 rat exposed to 200 R x-ray and killed 6 hours later. **(B)** Horizontal section from a similarly treated E15 rat. (3 µm methacrylate sections, toluidine blue stain.)

Days E16–E18

There is a marked change in cortical response to x-irradiation on E16. In the anterior cortex (Fig. 10–5A), darkly staining noncollapsing patches of surviving cells in the neuroepithelium (ne) alternate with collapsing areas where pyknotic cells spill into the lateral ventricle (lv). This patchy collapse is most pronounced in the medial and dorsal cortex; it is less obvious laterally where the cortical plate (CP) is beginning to form. There is no sign of neuroepithelial collapse in

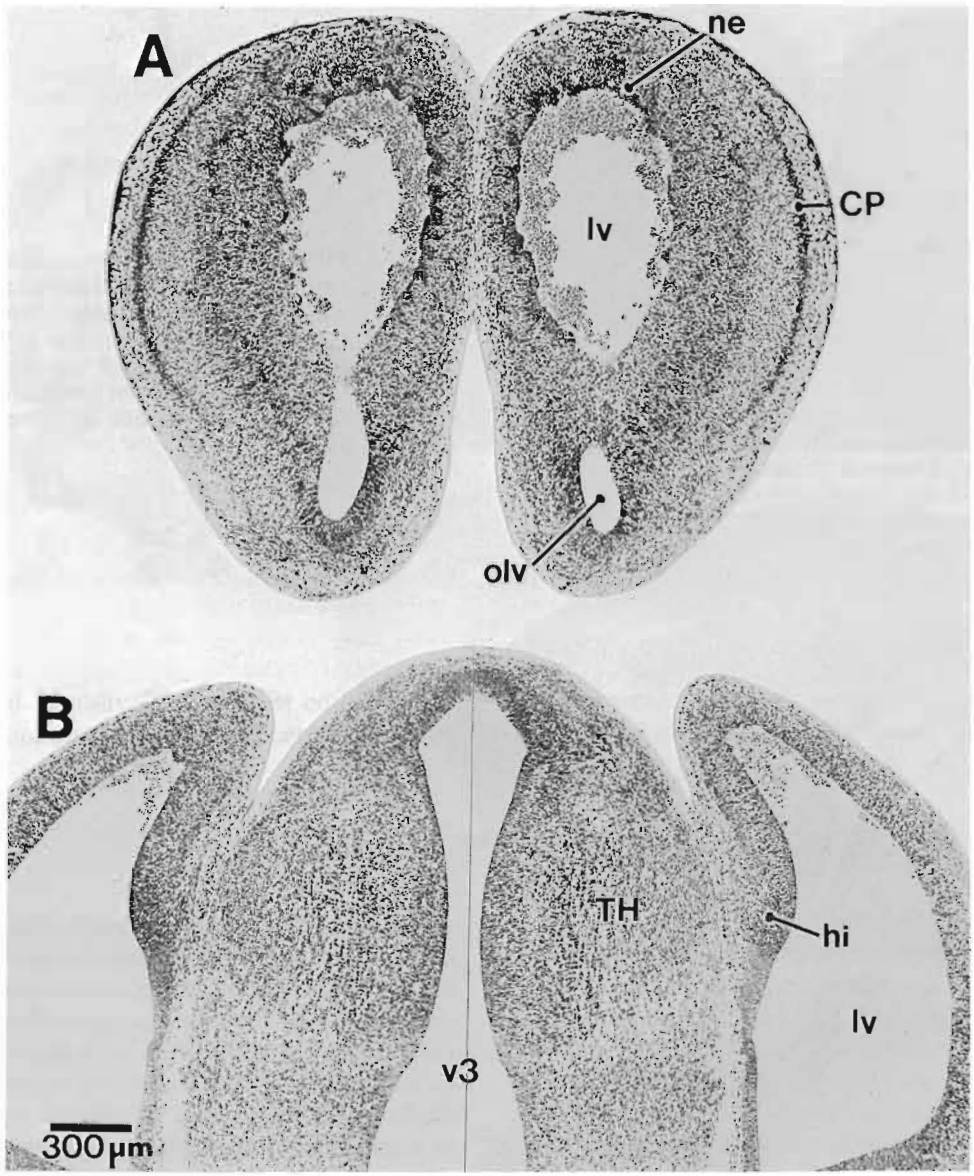

FIG. 10–5. An anterior **(A)** and a posterior **(B)** coronal section of the cortex from an E16 rat exposed to 200 R x-ray and killed 6 hours later. Note patchy collapse with spared islands of the neuroepithelium anteriorly. Posteriorly, collapse is limited to the dorsomedial wedge of the cortex; there is no neuroepithelial collapse laterally. (3 μm methacrylate sections, toluidine blue stain.)

the olfactory ventricle (olv). In the posterior cortex (Fig. 10–5B), neuroepithelial collapse is limited to the dorsomedial wedge; the lateral cortex shows no collapse. These observations suggest an posterior-to-anterior and a lateral-to-dorsal gradient in cortical neuroepithelial collapse that can also be seen in horizontal sections. In the dorsal cortex (Fig. 10–6A), patchy collapse is evident throughout from medial to lateral, and from anterior to posterior, the hippocampus (hi) excepted. In the lateral cortex (Fig. 10–6B), patchy collapse is pronounced anteriorly but there is only minimal collapse posteriorly in the occipital pole.

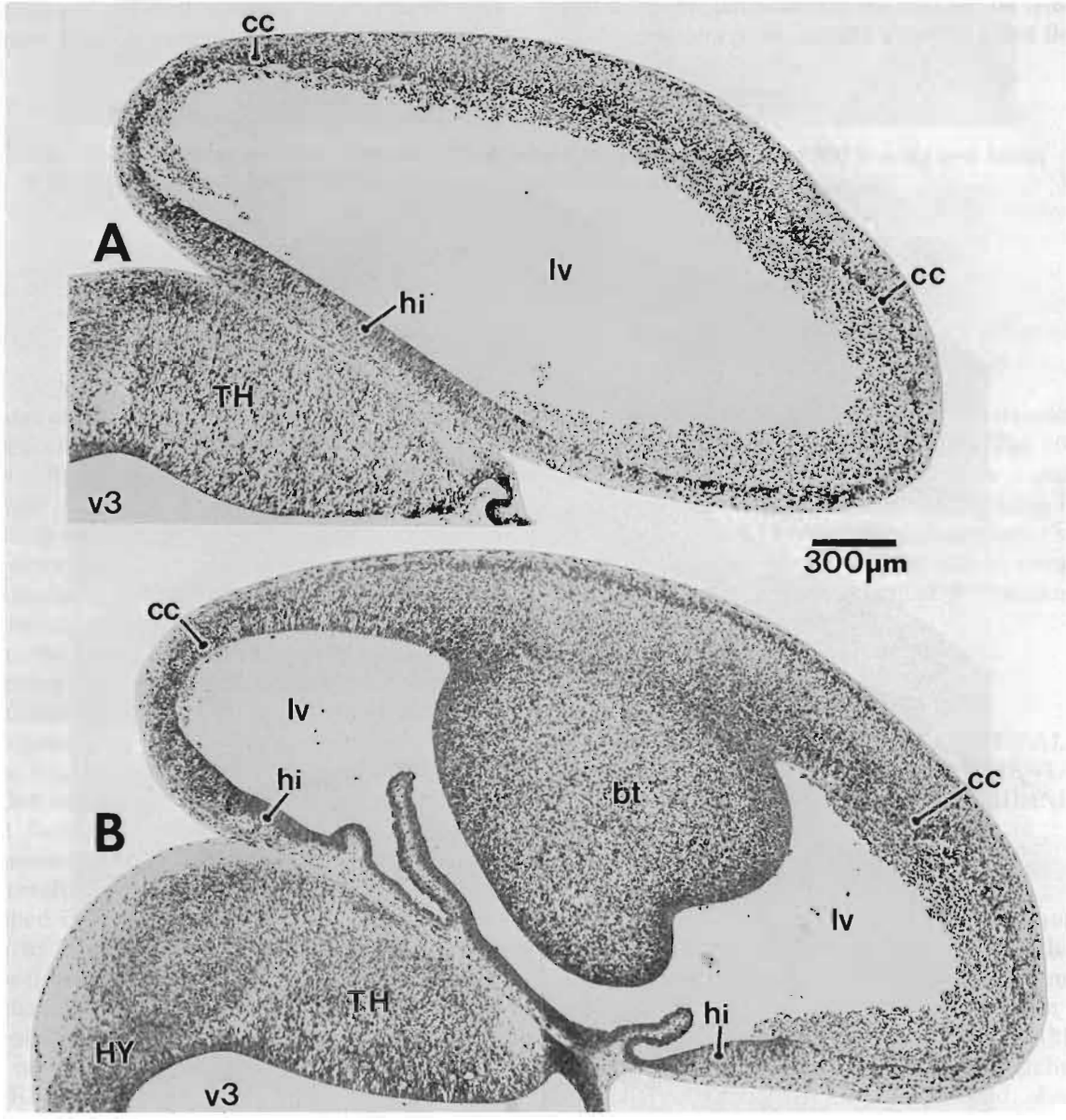

FIG. 10–6. Dorsal **(A)** and ventral **(B)** horizontal sections from an E16 rat exposed to 200 R x-ray and killed 6 hours later. Note patchy collapse through much of the dorsal cortex **(A).** In the lateral cortex **(B)** patchy collapse is limited to the anterior part. (3 μm methacrylate sections, toluidine blue stain.)

The patchy neuroepithelial collapse seen on E16 persists in the dorsomedial cortex, although to a progressively diminishing extent, through E17 and up to E18 (Fig. 10–7). On E16 (Fig. 10–7A), the surviving neuroepithelial patches are small and there is a large accumulation of pyknotic remains. By E17 (Fig. 10–7B), the persisting neuroepithelial patches have increased in size, but pyknotic debris is still abundant in the ventricle. Finally, by E18 (Fig. 10–7C), enough periventricular cells survive to form a nearly intact wall but the persistence of patchy collapse is suggested by small, intermittent clusters of pyknotic debris shed into the ventricle. However, an anterior coronal section (Fig. 10–8A) shows that the dorsomedial wedge of the cortex still has a copious amount of pyknosis.

Day E19

Although a high proportion of cortical cells are still killed by 200 R x-ray on E19 (and for several days thereafter), and a rare pyknotic fragment may be seen in the ventricle, there is no longer any sign of neuroepithelial collapse on this day even in the most radiosensitive dorsomedial region of the cortex (Fig. 10–8B).

Summary and Comments

Our observations indicate that the presumptive primordium of the cerebral cortex is more vulnerable to

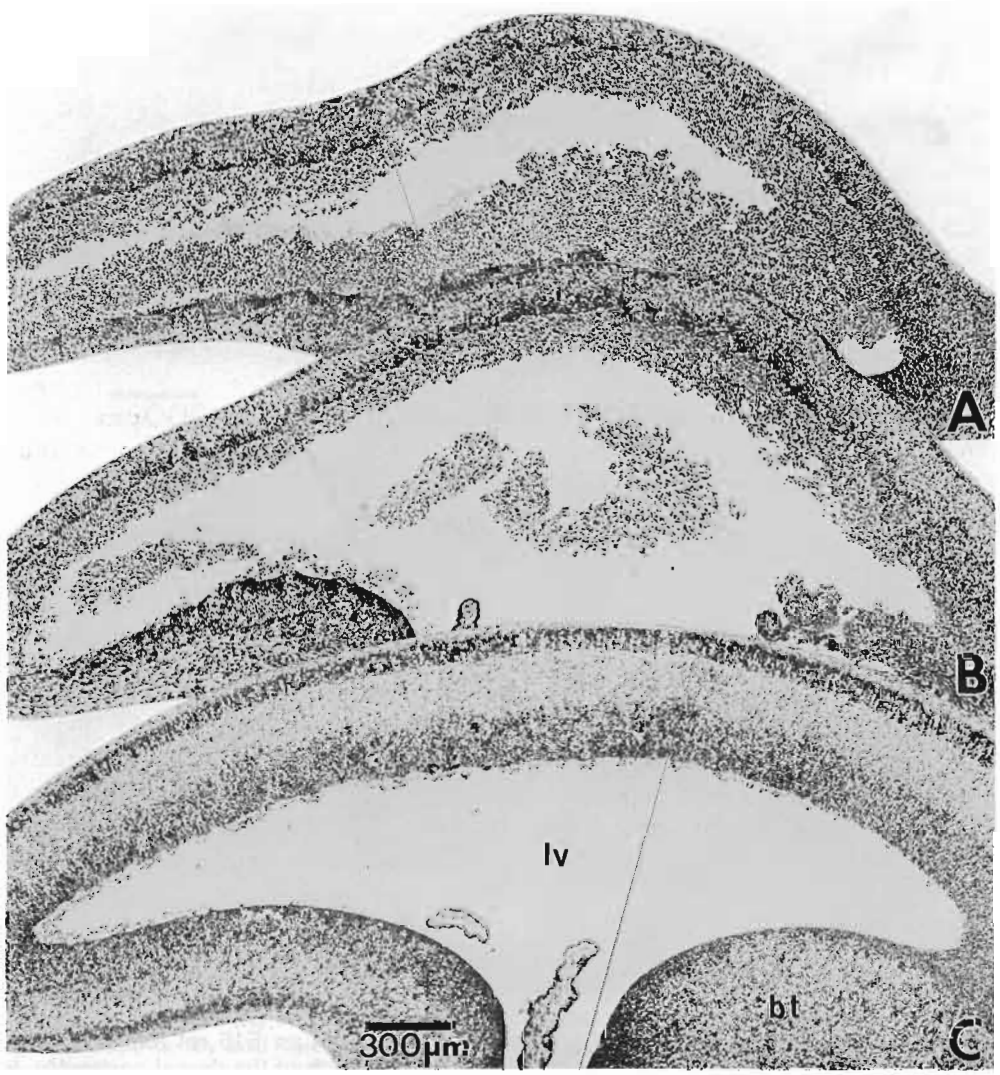

FIG. 10–7. Sagittal sections through the dorsomedial cortex in E16 **(A)**, E17 **(B)**, and E18 **(C)** rats that were exposed to 200 R x-ray and were killed 6 hours later. Note the decreasing magnitude of patchy collapse. (3 μm methacrylate sections, toluidine blue stain.)

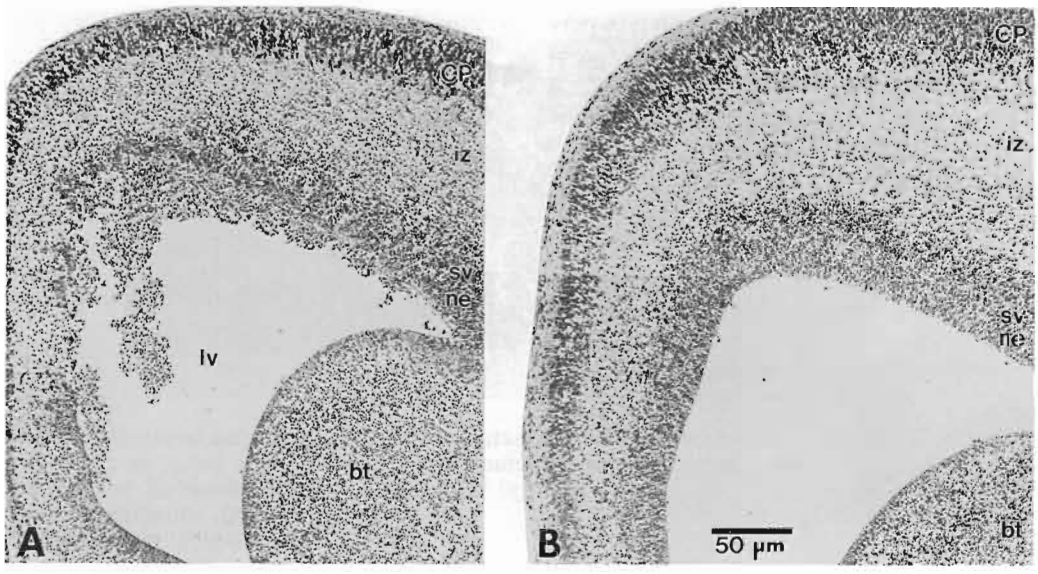

FIG. 10–8. Coronal sections from an E18 **(A)** and E19 **(B)** rat exposed to 200 R x-ray and killed 6 hours later. (3 μm methacrylate sections, toluidine blue stain.)

a single dose of 200 R x-ray than are other components of the telencephalon. Because the germinal matrix of the cortex collapses after irradiation while that of other telencephalic regions (e.g., the basal ganglia) do not, the long-term consequences of x-ray exposure should be more detrimental in the cortex than in the basal ganglia. Interesting in this context is the observation of Hicks and D'Amato (1961) that, several days after irradiation, the cortex is filled with islands, or rosettes, of reorganized neuroepithelium while the basal ganglia show a normal neuroepithelial lining. Apparently, the spared fragments of cortical neuroepithelium cannot regenerate a structurally normal germinal matrix. The regeneration of the cortical germinal matrix in a disorganized fashion must have devastating long-term consequences (see Section 10.6).

These results also indicate that three stages can be distinguished in the response of the cortical neuroepithelium to 200 R x-irradiation during its development. The first stage is on E13 (Fig. 10–2) when many neuroepithelial cells are killed and spill into the ventricle but others are spared so that the neuroepithelium does not completely disintegrate. During the second stage on E14 and E15 (Figs. 10–3 and 10–4), there is nearly complete destruction of stem cells and total collapse of the neuroepithelium. The third stage is characterized by the progressive sparing of neuroepithelial cells. This stage has two subdivisions that have different features in different areas of the developing cortex. During early stage 3, on E16–E18 (Fig. 10–7), only clumps of stem cells survive and there is patchy spillage of pyknosis into the ventricle. During late stage 3, on and after E19, enough periventricular stem cells survive to allow the ventricular wall to remain intact throughout the entire neocortical primordium.

10.2 RELATING CHANGES IN CORTICAL RADIOSENSITIVITY TO DEVELOPMENTAL CHANGES REVEALED WITH THYMIDINE AUTORADIOGRAPHY

Changes in neuroepithelial radiosensitivity and in the rest of the developing cortex can be related to changing cell labeling patterns revealed with [^{3}H]thymidine autoradiography. First, observations made in rats that were killed 2 hours after labeling with [^{3}H]thymidine provide some clues about the stage of patchy neuroepithelial collapse (early stage 3). Second, observations in embryonic rats killed 24 hours after the administration of [^{3}H]thymidine indicate that changes in cell kinetics can partially explain the remaining stages of neuroepithelial radiosensitivity (1, 2, and late 3).

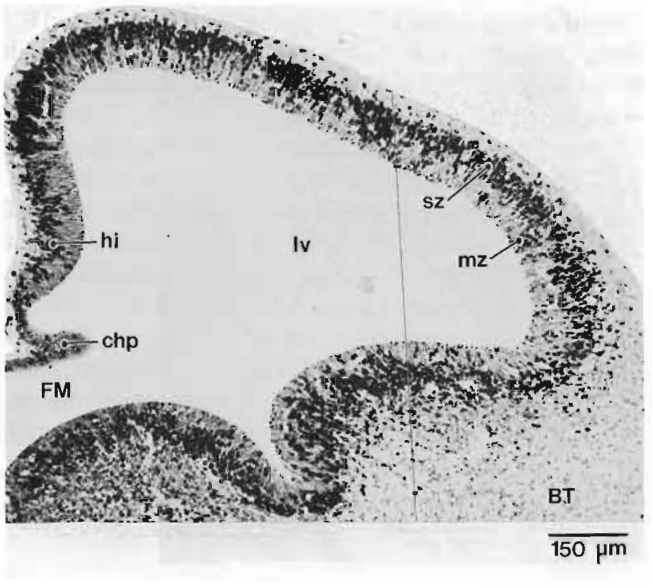

FIG. 10–9. Short-survival (2 hours) coronal autoradiogram from an E15 rat, showing the sawtooth pattern of cell labeling in the cortical neuroepithelium. (6 μm paraffin section, hematoxylin stain.)

10.2.1 Patchy Neuroepithelial Collapse in Relation to Cell Labeling in Thymidine Autoradiograms

Observations

Examination of short-survival (2 hours) [^{3}H]thymidine autoradiograms in an E15 embryo (Fig. 10–9) indicates that labeled cells in the synthetic zone do not form a continuous band in the cortical neuroepithelium but aggregate in patches reminiscent of bunches of grapes strung on a line. The labeled patches alternate with unlabeled cell clusters in and above the mitotic zone. The patches first appear 2 hours after [^{3}H]thymidine injections on E13 (Fig. 10–10A) but become more prominent on E14 (Fig. 10–10B) and E15 (Fig. 10–10C). They are still obvious on E16 (Fig. 10–12A). Al-

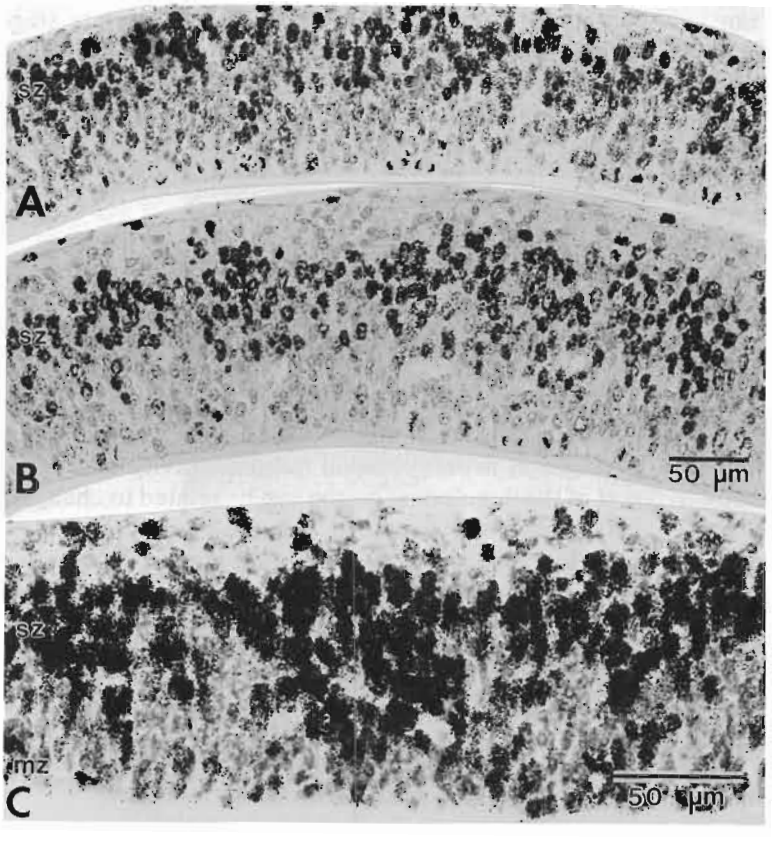

FIG. 10–10. Short-survival (2 hours) autoradiograms showing the pattern of neuroepithelial cell labeling in the cortex of rats that received [^{3}H]thymidine on E13 **(A)**, E14 **(B)**, and E15 **(C)**. The patchy distribution of labeled cells in the synthetic zone (sz) is evident. (**A–B,** 3 μm methacrylate sections, hematoxylin stain; **C,** 6 μm paraffin section, hematoxylin stain.)

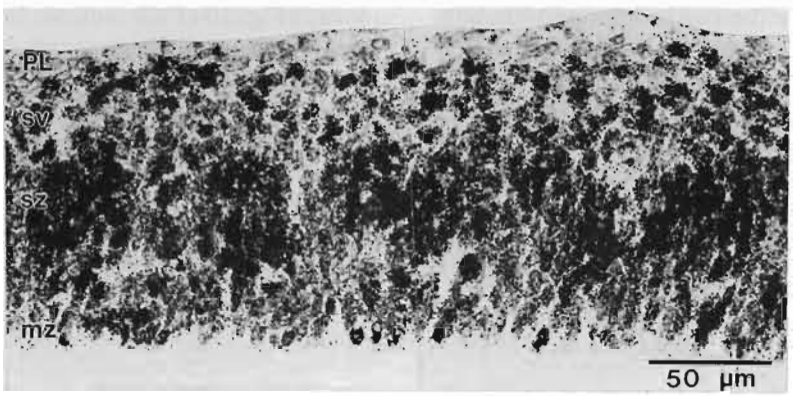

FIG. 10–11. Coronal autoradiogram of the dorsal cortex from a rat that received [^{3}H]thymidine on E15 and was killed on E16, showing the patchy arrangement of heavily labeled cells in the synthetic zone (sz) embedded in a matrix of lightly labeled cells. (6 μm paraffin section, hematoxylin stain.)

though clusters of labeled cells can be seen dorsomedially on E17, they are not as obvious as they were earlier. The patches are not seen on and after E18 because the segregation between the synthetic and mitotic zones is disappearing during that time (Chapter 4). While the patches are most obvious 2 hours after the injection of [^{3}H]thymidine, they can also be seen 24 hours later, as shown in a rat that received [^{3}H]thymidine on E15 and was killed on E16 (Fig. 10–11). However, after 24 hours heavily labeled patches alternate with lightly labeled patches. These observations are relevant here because they partially coincide with the patchy collapse of the neuroepithelium following x-irradiation. Patches of surviving cells are seen in the neuroepithelium on E16 and E17 in widespread areas of the cortex and persist in the dorsomedial cortex until E18. In low magnification coronal sections from rat embryos on E16 for example, the size of the alternating unlabeled cell clusters seen near the ventricular lumen in a [^{3}H]thymidine autoradiogram (Fig. 10–12A) is similar to the size of the surviving cell patches seen in the neuroepithelium following x-irradiation (Fig. 10–12B). A higher magnification series of E16 embryos shows a methacrylate-embedded speci-

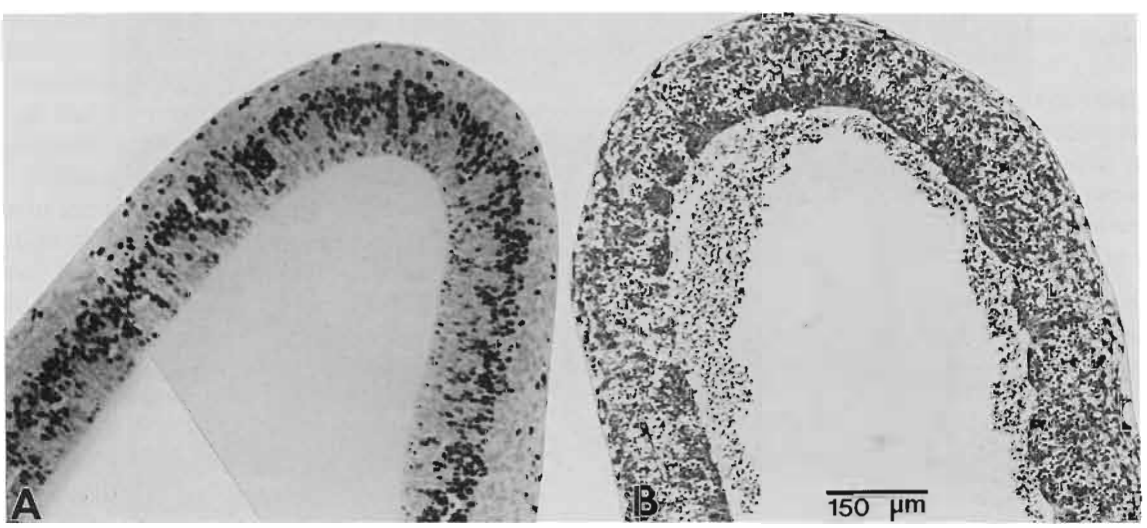

FIG. 10–12. (A) Short-survival (2 hours) autoradiogram of a coronal segment of the cerebral cortex of an E16 rat labeled with [^{3}H]thymidine. **(B)** Corresponding section from an E16 rat killed six hours after exposure to 200 R x-ray. Note the similar periodicities in the pattern of neuroepithelial labeling and alternation of radiosensitive (collapsing) and radioresistant (noncollapsing) patches of the neuroepithelium. (**A,** 6 μm paraffin section, hematoxylin stain; **B,** 3 μm methacrylate section, toluidine blue stain.)

men (Fig. 10–13A) where the cortical neuroepithelium appears completely homogeneous. But the patchy labeling pattern 2 hours after the injection of [^{3}H]thymidine (Fig. 10–13B) and the alternating array of surviving and killed cells 6 hours after exposure to x-ray (Fig. 10–13C) indicate that the two experimental methods reveal hidden cellular heterogeneity in the neuroepithelium. However, the question remains whether these two methods (x-ray exposure versus [^{3}H]thymidine autoradiography) point to the same kind

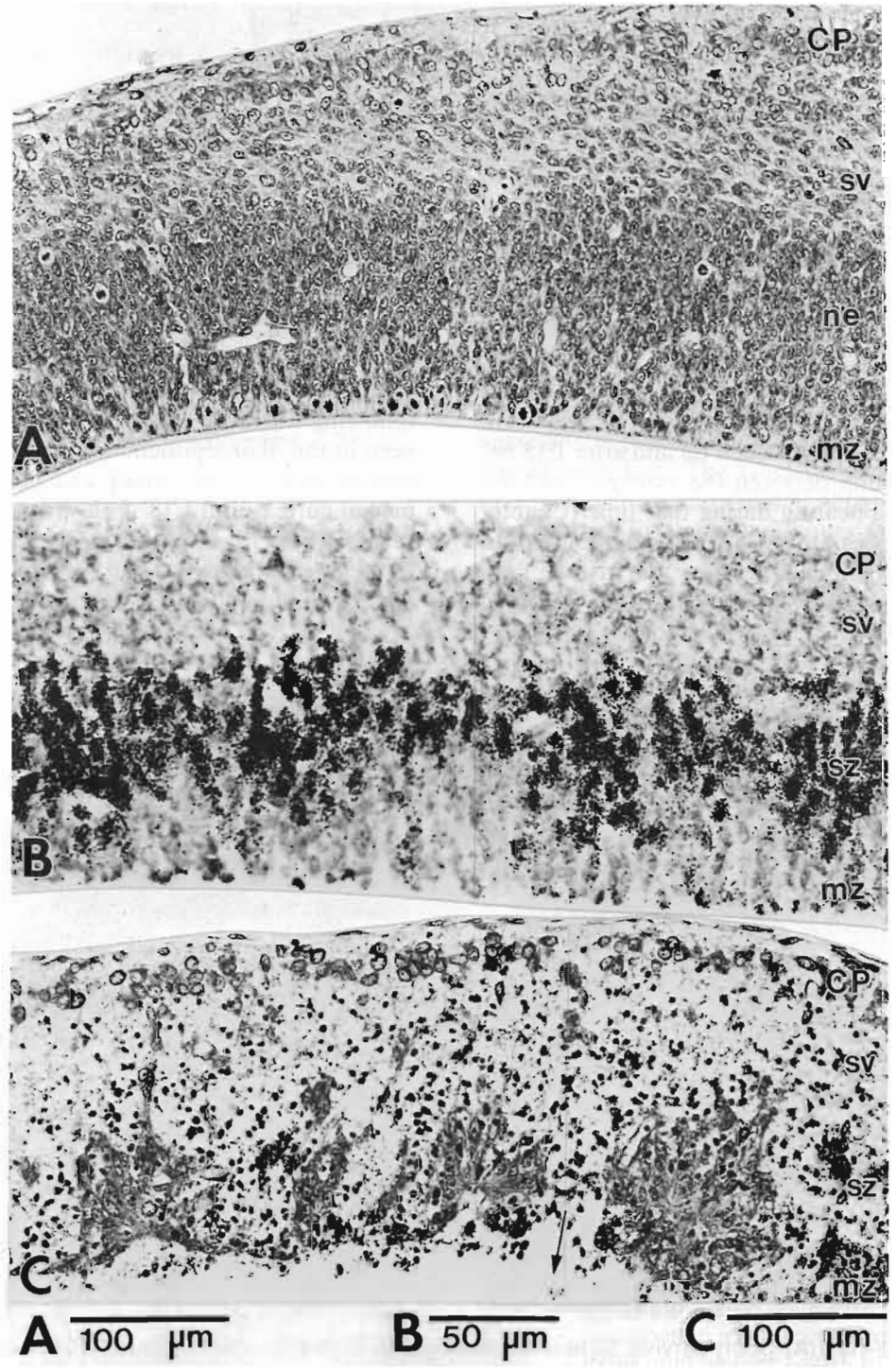

FIG. 10–13. A comparison of the neuroepithelium in E16 rats without experimental treatment **(A),** in an autoradiogram 2 hours after injection of [^{3}H]thymidine **(B),** and 6 hours after x-irradiation **(C).** (**A, C,** 3 µm methacrylate sections, toluidine blue stain; **B,** 6 µm paraffin section, hematoxylin stain.)

of heterogeneity. The answer is not certain, because the temporal correlation between the two sets of observations is not exact. The autoradiographic patches appear earlier and last for 4 days (E13 to E17), while the x-ray-induced patches appear later and last for only 3 days (E16 to E18).

Interpretation

There are several possible interpretations of these observations. From the perspective of cell kinetics, the alternating clusters of labeled and unlabeled cells could be composed either of fast-cycling (labeled) and slow-cycling (unlabeled) cells or, alternatively, of proliferative (labeled) and postmitotic (unlabeled) cells. Intuitively, fast cycling cells should be more radiosensitive than slow cycling cells, and proliferative cells should be more radiosensitive than postmitotic cells. From the perspective of cell commitment, the alternating clusters may be the segregated stem cells of neurons or glia, with one of them being more radiosensitive than the other (as well as each having different kinetic properties). A final possibility is that the patchy labeling pattern and the patchy collapse in the neuroepithelium is related to the columnar organization of the mature cortex. The rationale for considering each of these possibilities is given below.

Are the Segregated Cells Fast-Cycling or Slow-Cycling?

It has been reported that the rat cortical neuroepithelium is composed of fast-cycling and slow-cycling cells (Waechter and Jaensch, 1972). There is evidence that the lengthening of the cell cycle is due to the prolongation of the G1 (postmitotic, presynthetic) phase (Kaufman, 1968; Schultz and Korr, 1981). As a consequence of interkinetic nuclear migration, slow cycling cells in the G1 phase would tend to linger in the lower portion of the neuroepithelium, beneath the synthetic zone. In fact, the alternation of unlabeled and labeled patches is most pronounced in the lower portion of the neuroepithelium (Figs. 10–10 and 10–11). If this interpretation is correct, the patchy labeling pattern in short-survival autoradiograms might indicate that the fast-cycling cells (those more likely to be labeled by a brief exposure to [^{3}H]thymidine) and the slow-cycling cells (those less likely to be labeled) aggregate in separate compartments in the cortical neuroepithelium. The lower portion of the neuroepithelium also has alternating radioresistant and radiosensitive patches following x-irradiation, while the upper portion, the synthetic zone, has a continuous band of pyknosis (Figs. 10–13C).

Are the Segregated Cells Proliferating or Postmitotic?

Another possibility is that a fair proportion of the unlabeled cells seen in short-survival autoradiograms are not slow-cycling cells but are postmitotic cells ready to leave the neuroepithelium. This is supported by the observation that, in young embryos killed 24 hours after the administration of [^{3}H]thymidine, there are no unlabeled cells present in the neuroepithelium (Fig. 10–11). If the original unlabeled patches were composed of slow-cycling, proliferative cells, their progeny should be unlabeled in the neuroepithelium. Instead, unlabeled cells appear outside of the neuroepithelium in the primordial plexiform layer (PL, Fig. 10–11).

Are the Segregated Cells Neuronal or Glial Precursors?

The possibility that the aggregates of fast- and slow-cycling cells and of radiosensitive and radioresistant cells represent two different stem cell populations (neurons versus glia) deserves serious consideration. Evidence for the alternation of neuronal and glial stem cells in the neuroepithelium is indicated by immunocytochemical evidence in the developing primate cortex (Levitt et al., 1983) and in the developing rodent cortex (Misson et al., 1988a, 1988b). Protooncogene expression also reveals heterogeneity between radial glia and surrounding nonstained proliferating cells (Johnston and van der Kooy, 1989). Earlier studies with x-irradiation have shown that the proliferating precursors of glial and ependymal cells are more radioresistant than are neurons (Altman et al., 1968). If that is true, the surviving patches of cells after x-irradiation could represent glial or ependymal elements, while the collapsing patches would predominantly contain stem cells of neurons. The increasing radioresistance of the cortical neuroepithelium in older embryos in association with the decline of neurogenesis and increase in gliogenesis supports that hypothesis.

Is Cellular Segregation a Precursor of Columnar Cortical Organization?

We have considered the possibility that the predominantly vertically aligned patches in the cortical neuroepithelium are the primordia of the structural columns (e.g., Colonnier, 1966; von Bonin and Mehler, 1971) and functional columns (e.g., Mountcastle, 1957; Hubel and Wiesel, 1965) of the mature cortex. However, the large size of the neuroepithelial patches (which, as proliferative elements, should give rise to even larger neuronal populations) speaks against that

interpretation because the columns in the adult cortex are quite narrow.

10.2.2 Neuroepithelial Collapse in Relation to Cell Labeling 24 Hours after the Administration of Tritiated Thymidine

Observations

The first stage of moderate destruction of neuroepithelial cells is found 6 hours after x-irradiation on E13 (Figs. 10–2 and 10–14B) and correlates with the primordial labeling pattern seen in [^{3}H]thymidine autoradiograms from rats injected on E12 and killed on E13 (Fig. 10–14A). The primordial pattern is characterized by no bands of heavily labeled cells in the neuroepithelium 1 day after [^{3}H]thymidine injection, presumably because most of the stem cells are cycling at a relatively rapid rate (Chapter 4). A matched section from an E13 rat that was exposed to 200 R x-ray (Fig. 10–14B) shows that this is also the period during which a fair proportion of the neuroepithelial cells are spared. The presence of mitotic figures in the neuroepithelium (*arrows*, Fig. 10–14B) suggests that the cells situated near the lumen (those forming the lining of the ventricle) are no more affected than the cells farther away from the lumen. However, the surviving neuroepithelial cells do not form isolated patches where the lumen of the lateral ventricle should be but are displaced much farther upward, above the pyknotic debris that collapses into the ventricle (col, Fig. 10–14B). The stage of moderate destruction also occurs prior to peak days of cortical neurogenesis because most of the Cajal-Retzius cells are not generated until E14 (Chapter 3).

The second stage of total neuroepithelial collapse is found 6 hours after x-irradiation on E14 (Fig. 10–3) and E15 (Figs. 10–4 and 10–15B) and loosely correlates with the early labeling pattern of the cortical neuroepithelium seen in autoradiograms from rats killed 24 hours after injections of [^{3}H]thymidine on E14 and E15 (Chapter 4). Rats injected on E14 that survived to E15 have heavily labeled cells in the upper one-third of the cortical neuroepithelium, lightly labeled cells in the lower two-thirds (up,h and lo,l, Fig. 10–15A). In a corresponding section from a rat that survived for 6 hours after irradiation on E15, all cells are killed in the collapsed neuroepithelium, and the pyknotic debris is shed into the ventricle (col, Fig. 10–15B). These observations suggest that lightly labeled, fast-cycling cells near the ventricle in the neuroepithelium are all killed by the x-ray exposure. The only surviving cells are those in layer I (the presumed Cajal-Retzius cells) and possibly a fraction of the cells in the upper neuroepithelium that tend to be heavily labeled (up,h, Fig. 10–15B). The latter may be either slowly cycling mitotic cells or sequestered postmitotic neurons that are ready to migrate to the primordial plexiform layer.

The third stage of neuroepithelial sparing is found after x-irradiation on E16 and thereafter, when the surviving cells form either isolated patches or a continuous band at the edge of the ventricle (Figs. 10–5 to 10–8). That correlates with the appearance of the late labeling pattern of the cortical neuroepithelium seen in autoradiograms from rats killed 24 hours after in-

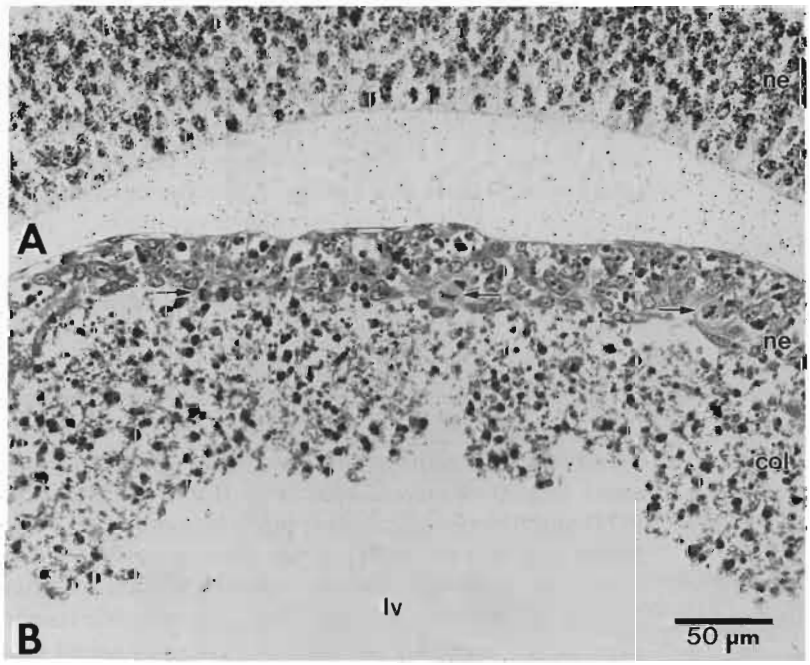

FIG. 10–14. (A) Coronal autoradiogram from a rat that received [^{3}H]thymidine on E12 and was killed on E13. **(B)** Corresponding section from an E13 rat that was exposed to 200 R x-ray and was killed 6 hours later. Arrows point to spared mitotic cells near the lumen. (3 μm methacrylate sections; **A,** hematoxylin stain; **B,** toluidine blue stain.)

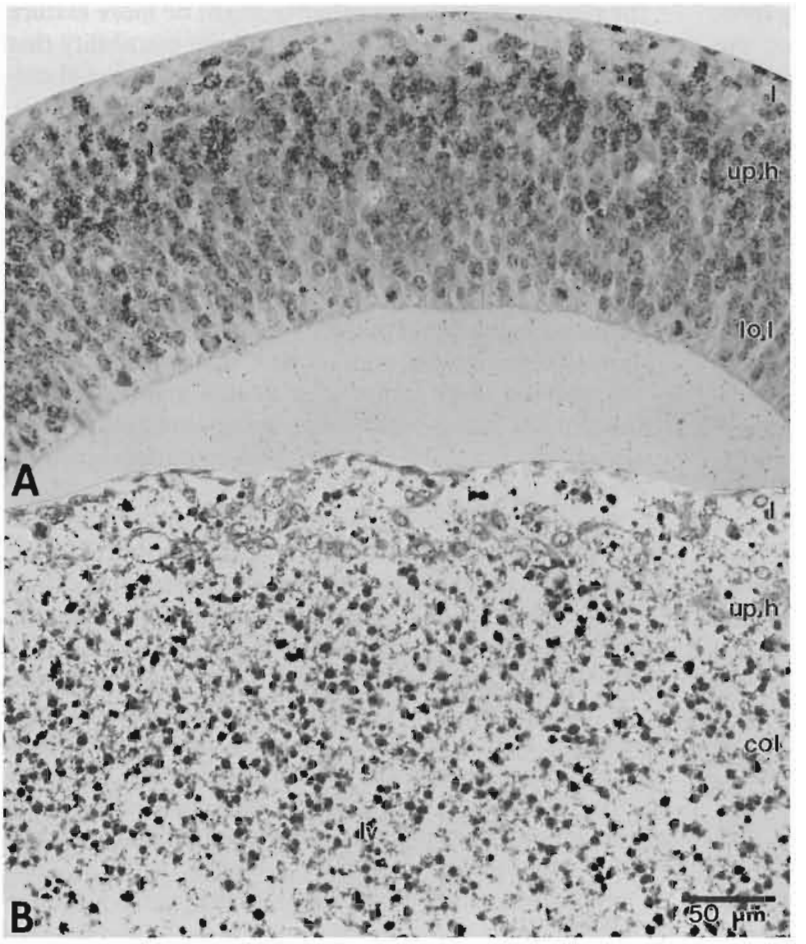

FIG. 10–15. (A) Coronal autoradiogram from a rat that received [^{3}H]thymidine on E14 and was killed on E15. **(B)** Corresponding section from an E15 rat that was exposed to 200 R x-ray and was killed 6 hours later. (3 μm methacrylate sections, **A,** hematoxylin stain; **B,** toluidine blue stain.)

jections of [^{3}H]thymidine on E16 to E20 (Chapter 4). Although pyknotic debris is still abundant in the neuroepithelium on E19 (Fig. 10–8B), the cells that line the ventricle are radioresistant (survive) and form a barrier that prevents the dead cells from being shed into the ventricle. It can be seen in a corresponding autoradiogram from a rat that received [^{3}H]thymidine on E18 and was killed on E19 (Fig. 10–16) that the neuroepithelium in the dorsomedial cortex shows the typical late-labeling pattern with heavily labeled cells concentrated near the lumen and lightly labeled cells above them (lo,h and up,l, Fig. 10–16). The heavily labeled cells (presumably slowly cycling precursors of glia and ependymal cells) are apparently the surviving radioresistant elements that now prevent neuroepithelial collapse.

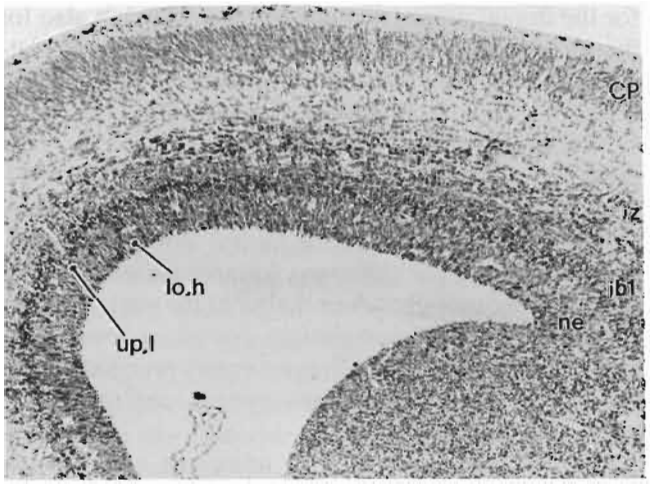

FIG. 10–16. Coronal autoradiogram from a rat that received [^{3}H]thymidine on E18 and was killed on E19. Note that heavily labeled cells line the ventricle dorsomedially (lo,h and up,l). (6 μm paraffin section, hematoxylin stain.)

Comments

These observations indicate that there is a correlation between the progressive transformation of the cortical neuroepithelium seen with [^{3}H]thymidine autoradiography and its changing radiosensitivity. Stage 1 of neuroepithelial radiosensitivity (early moderate sparing) coincides with the primordial labeling pattern (no band of heavily labeled cells 24 hours after injection). Stage 2 of neuroepithelial radiosensitivity (total collapse) coincides with the early pattern, where the heavily labeled cells form a band above the lightly labeled cells.

Finally, stage 3 of neuroepithelial radiosensitivity (progressive sparing) coincides with the reversal of the neuroepithelium from the early- to the late-labeling pattern where the heavily labeled cells form a band below the lightly labeled cells. Just as the reversal of neuroepithelial labeling sweeps across the cortex from ventrolateral to dorsomedial (Chapter 4), so also does neuroepithelial radioresistance.

The progressive neuroepithelial radioresistance is manifested in the anterior cortex by a change from patchy collapse to no collapse. On E16 and E17 for example, there is widespread patchy neuroepithelial collapse in the anterior part of the neocortical primordium. By E18, ventrolateral parts of the anterior cortical neuroepithelium remain intact after x-irradiation, and only the dorsomedial area shows patchy collapse. By E19, the anterior dorsomedial ventricular wall is intact after exposure to x-irradiation. The pattern is different in the posterior cortex, however. As early as E16, the posterior cortical neuroepithelium has only a small area of collapse in the dorsomedial wedge, and the remainder is intact.

10.3 THE POSSIBLE CELLULAR BASIS OF THE REGIONAL DIFFERENCES IN PATCHY NEUROEPITHELIAL COLLAPSE

As we have noted in Section 10.1, the patchy collapse of the cortical neuroepithelium is more pronounced in the anterior than it is in the posterior cortex (Fig. 10–5A,B), and there is also a gradient from ventrolateral to dorsal (Fig. 10–6A,B). The regional differences in patchy collapse of the neuroepithelium is illustrated in a series of low magnification coronal sections of a rat that was exposed to 200 R x-ray on E16 and was killed 6 hours later (Figure 10–17). In the presumptive frontal cortex (Fig. 10–17A), the entire neuroepithelium shows patchy collapse, and pyknotic cells fill the lateral ventricle (lv). At this level the neuroepithelium surrounding the olfactory ventricle (olv) is spared. More posteriorly in the frontal cortex (Fig. 10–17B), patchy neuroepithelial collapse is limited to the medial and dorsal cortex (*arrows*); the neuroepithelium of the lateral cortex does not collapse nor does the neuroepithelium of the basal telencephalon (BT) and septum (SE). The same pattern prevails farther posteriorly at midcoronal levels (Figs. 10–17C,D) but there is gradual shrinkage of the collapsing zone to the dorsal and dorsomedial cortex (*small arrows*). Finally, neuroepithelial collapse is limited to the dorsal wedge of the cortex in the most posterior section (*arrow,* Fig. 10–17E).

Since neuroepithelial collapse is a phenomenon seen only during the early period of cortical development, the regions showing no collapse might be more mature than those that do. We entertained the possibility that the regional differences in patchy neuroepithelial collapse reflect regional gradients in cortical maturation. There is a positive correlation in the medial-lateral plane because patchy collapse is more prominent in the late maturing dorsal and dorsomedial areas than it is in the earlier maturing ventrolateral and lateral areas. However, the regional differences in patchy collapse in the anterior-posterior plane are contrary to the maturation gradients in the developing neocortex. The earlier maturing anterior cortex (Chapters 2 and 3) would have to be interpreted as less mature because the patchy collapse is more pronounced and widespread there than it is in the later maturing posterior cortex (compare Fig. 10–17A and E).

The discrepancy between cortical maturation and neuroepithelial collapse is further shown on E16 by the absence of a relationship between the extent of cortical plate formation (a sign of maturity) and the extent of patchy neuroepithelial collapse produced by x-irradiation (a sign of immaturity). In the early maturing frontal cortex, where a thin cortical plate has already formed laterally (CP, Fig. 10–17A), there is patchy neuroepithelial collapse in the lateral wall. In the later maturing posterior cortex, where the cortical plate has not yet formed, there is no neuroepithelial collapse (Fig. 10–17E).

An alternative interpretation is that patchy neuroepithelial collapse is more pronounced in those areas that are the presumed sources of laterally migrating neurons. We have provided evidence in Chapters 2 and 9 that the neuroepithelium of the anterior cortex progressively shrinks in a dorsomedial direction in association with the growth of the basal ganglia. Since the anterodorsal cortical neuroepithelium has regressed from the lateral wall, it is supplying neurons not only for the dorsal areas (that migrate radially) but also for the lateral and ventrolateral areas (that migrate laterally) (see Chapter 9). A unit area of the anterodorsal cortical neuroepithelium might contain a higher concentration of radiosensitive neuronal precursor cells relative to the radioresistant nonneuronal precursor cells. Because the posterodorsal cortical neuroepithelium does extend into the lateral and ventrolateral wall, it only supplies neurons for areas directly above (that migrate radially). A unit area of the posterodorsal cortical neuroepithelium might contain a lower concentration of radiosensitive neuronal precursor cells relative to the radioresistant nonneuronal precursor cells.

This hypothesis leaves two questions unanswered. First, why is there patchy neuroepithelial collapse anterolaterally in the frontal cortex (Fig. 10–17A), and, second, why is there neuroepithelial collapse dorso-

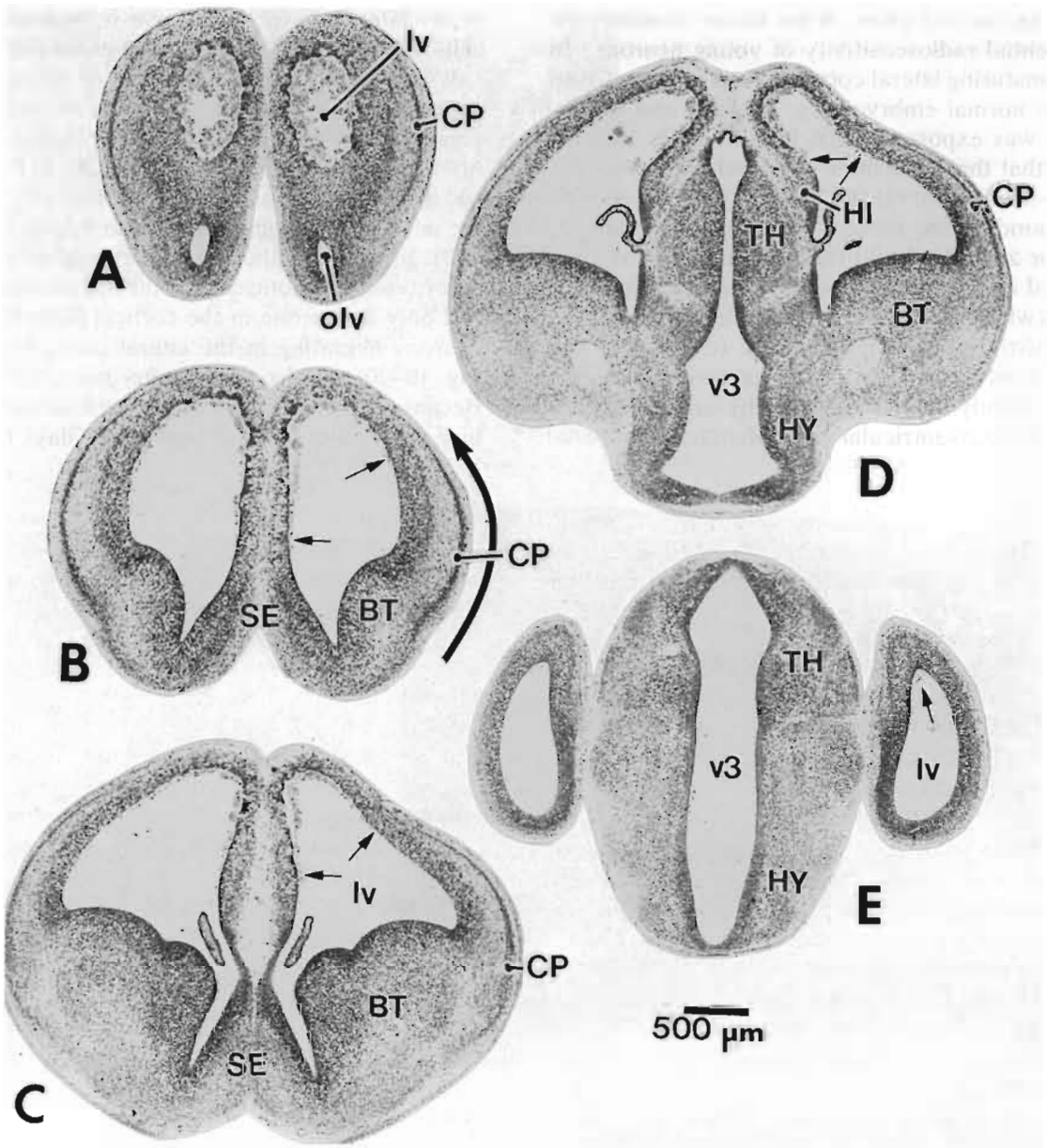

FIG. 10–17. Regional differences in the patchy collapse of the cortical neuroepithelium (*arrows*) from rostral to caudal **(A–E)** in an E16 rat that was killed 6 hours after exposure to 200 R x-ray. (3 μm methacrylate sections, toluidine blue stain.)

medially in the posterior cortex (Fig. 10–17E)? In trying to answer these questions we raise the possibility that, in addition to the long distance migration of young cortical neurons from dorsal to lateral anteriorly (by way of the prominent lateral cortical stream), there may also be other migrations in progress, perhaps from the anterior cortical neuroepithelium to posterior areas and from the dorsomedial posterior cortical neuroepithelium to anterior areas (such migrations have been noted by Austin and Cepko, 1990).

10.4 THE DIFFERENTIAL RADIOSENSITIVITY OF MIGRATING NEURONS: THE FACTOR OF AGE

Pyknotic cells abound not only in the neuroepithelium but also throughout the subventricular and intermediate zones, and some are even killed in the cortical plate (Fig. 10–1). Evidently, many migrating neurons and possibly some of the differentiating neurons remain radiosensitive. However, other cells are spared in the subventricular and intermediate zones and many

more in the cortical plate. What factor accounts for the differential radiosensitivity of young neurons? In the early-maturing lateral cortex on E17, a comparison between a normal embryo (Fig. 10–18A) and an embryo that was exposed to 200 R x-ray (Fig. 10–18B) indicates that there are three strata where many cells survive x-irradiation: (1) the base of the neuroepithelium surrounding the mitotic zone (mz), (2) the subventricular zone (sv), and (3) the cortical plate (CP). The spared cells in the neuroepithelium correspond to the region where cells are heavily labeled 24 hours after the administration of [^{3}H]thymidine (Chapter 4) and are presumably precursors of nonneuronal elements (glia and ependymal cells). But why are many cells spared in the subventricular zone when few are spared in the intermediate zone above it, and why do some cells of the cortical plate remain radiosensitive?

We suggest that the regional differences in radiosensitivity are related to the presumptive age of young neurons irrespective of their locations. After x-ray exposure on E18, the dorsal cortex (Fig. 10–19A) has a fair accumulation of pyknotic cells not only in the intermediate zone (iz) but also in the cortical plate (CP). In contrast, the lateral cortex (Fig. 10–19B) has many fewer pyknotic cells in the intermediate zone (iz) and only a rare one in the cortical plate (CP). Young neurons migrating in the lateral cortical stream (lcs, Fig. 10–20) are also spared after x-irradiation on E18. Because the newly arriving neurons in the lateral cortical plate have spent at least 1 or 2 days migrating in

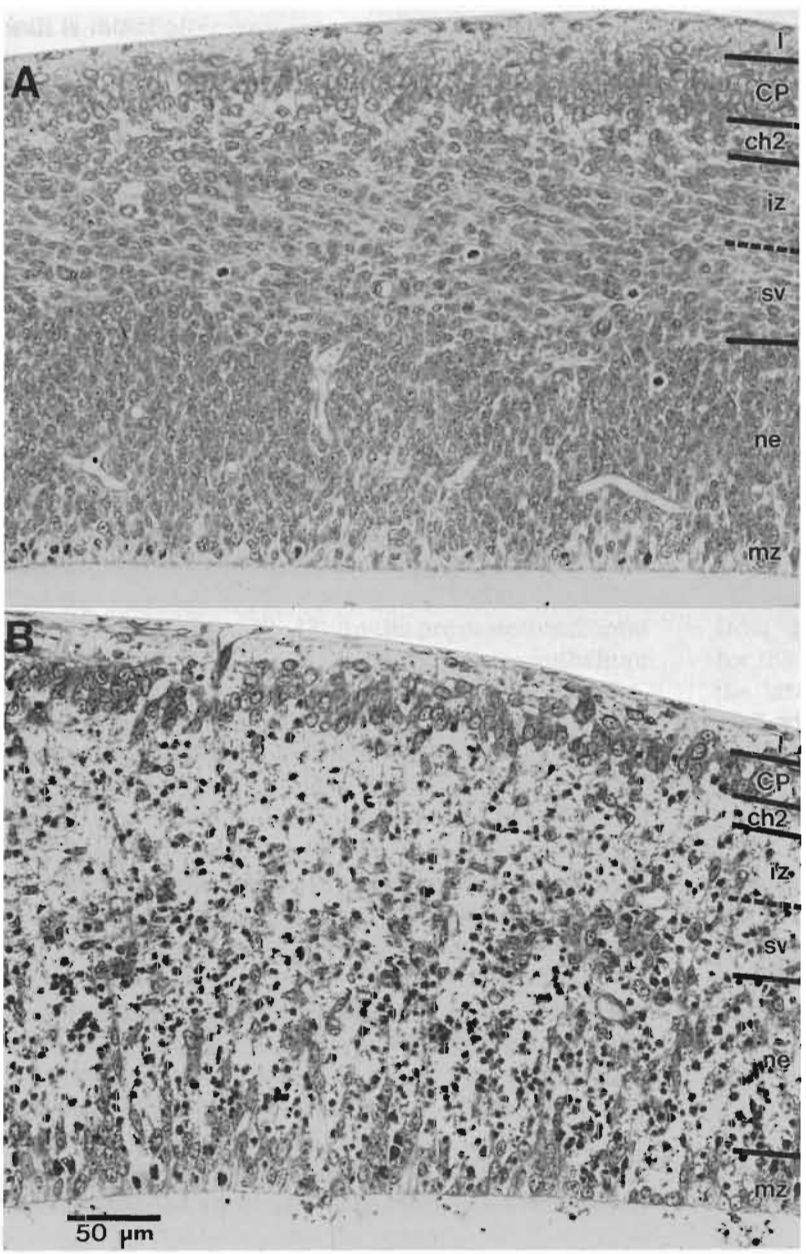

FIG. 10–18. Methacrylate sections of the neocortex from a normal E17 rat **(A)** and from a rat of the same age that was exposed to 200 R x-ray and was killed 6 hours later **(B).** Note the three bands with surviving cells in the mitotic zone (mz) of the neuroepithelium, in the subventricular zone (sv), and in the cortical plate (CP). (3 μm methacrylate sections, toluidine blue stain.)

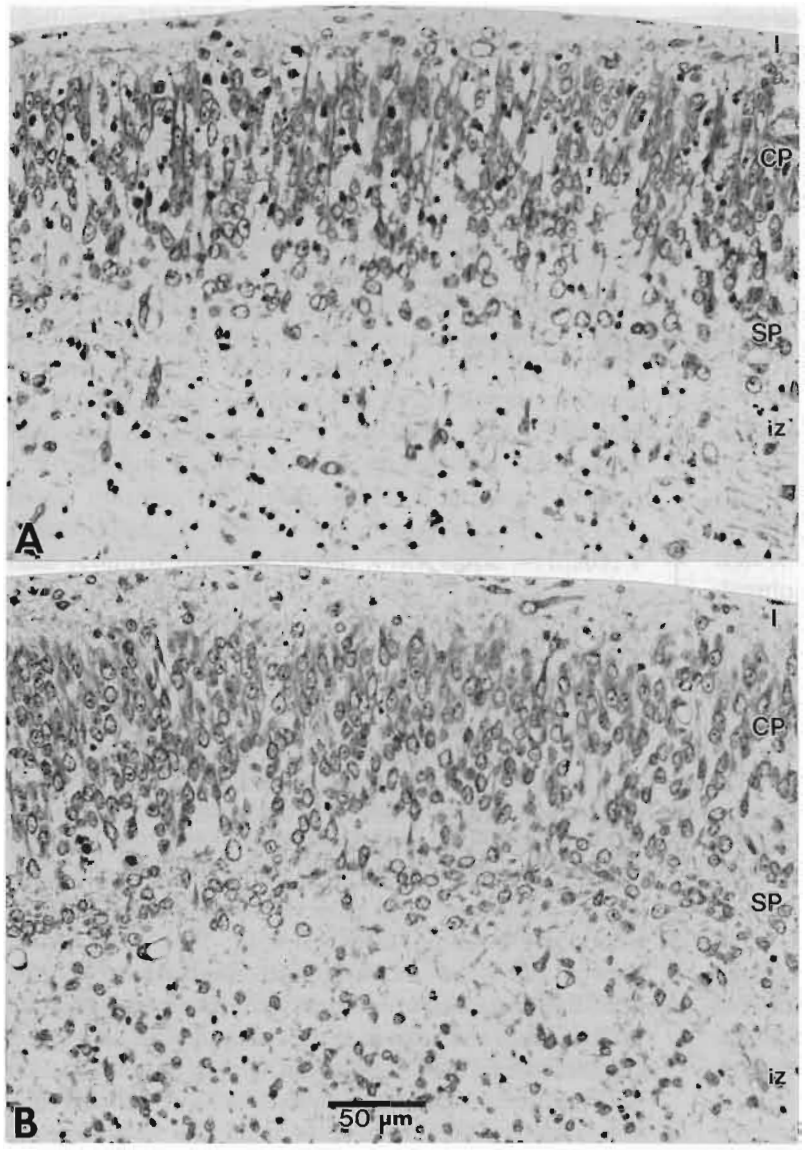

FIG. 10–19. Portions of the dorsal neocortex **(A)** and the lateral neocortex **(B)** within the same section from an E18 rat that was exposed to 200 R x-ray and was killed 6 hours later. Note the fair concentration of pyknotic cells in the intermediate zone (iz) and the cortical plate (CP) dorsally **(A)** and their paucity laterally **(B).** (3 μm methacrylate section, toluidine blue stain.)

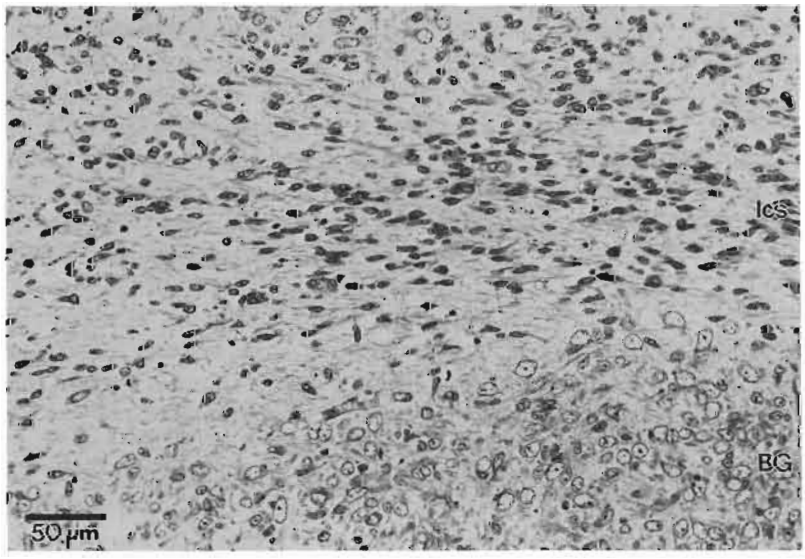

FIG. 10–20. The lateral cortical stream (lcs) from the same section shown in Fig. 10–19. Note the paucity of pyknotic cells.

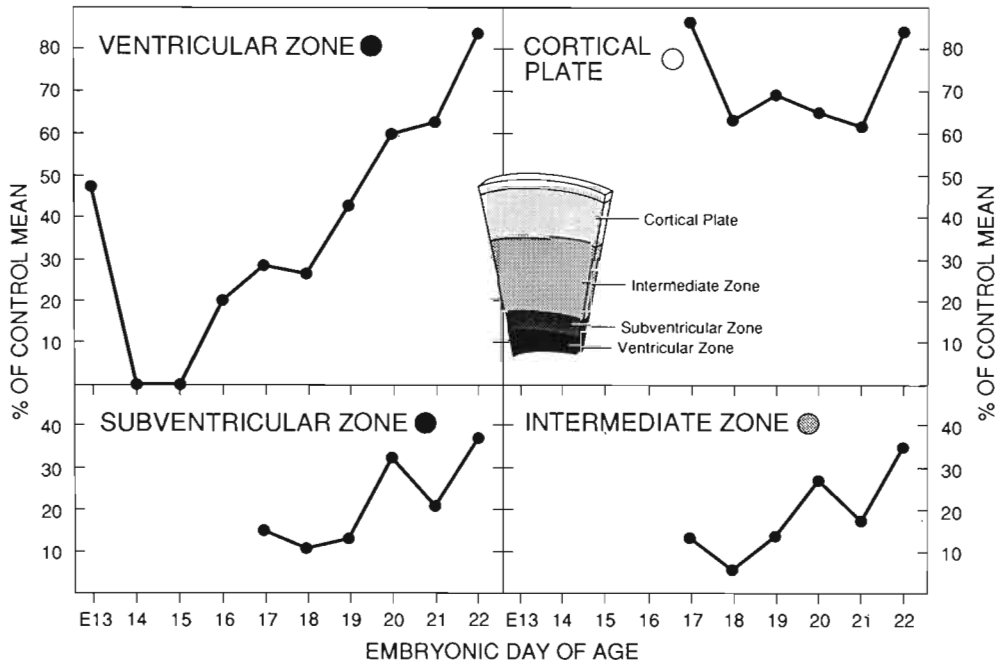

FIG. 10–21. The proportions of cells surviving 6 hours after an exposure to 200 R x-rays. For each experimental animal, the proportion of surviving cells was equal to the number of cells divided by the mean number of cells in the control group times 100; averages for the experimental groups are shown in the graph. Note that pyknotic debris was not quantified, only intact and normal cells. In the ventricular zone (*upper left*) radioresistance increases during embryonic development. Cells are highly radiosensitive throughout development in the subventricular and intermediate zones (two bottom graphs), while a majority of the cortical plate cells are radioresistant (*upper right*).

the lateral cortical stream, they are older than the newly arriving neurons in the dorsal cortical plate that have spent one day or less migrating directly radially (Chapter 9). That age difference may account for the differential radiosensitivity of the dorsal versus lateral cortical neurons. The spared cells in the subventricular zone may be those that are migrating laterally.

10.5 CHANGING RADIOSENSITIVITY OF DIFFERENT CELLULAR COMPONENTS OF THE DEVELOPING CORTEX: A QUANTITATIVE ANALYSIS

10.5.1 Steps in Data Collection and Analysis

Differences in the number of normal cells between control and x-irradiated rats were analyzed in sagittal sections of the dorsomedial neocortex from E13 to E22.[1] The ventricular zone (neuroepithelium) was studied throughout the entire observation period. Since the subventricular zone, the intermediate zone, and the cortical plate are not distinct in the dorsal neocortex until E17, quantification in those layers began then. In both control and experimental animals all cells were counted using a 40× objective and a 10 × 10 ocular grid that delimited a total area of 0.333 mm^2 at a final magnification of 625×. In animals that had been exposed to x-ray, only surviving cells were counted. (The number of pyknotic fragments were not counted since there may be several of them for each killed cell.) The total number of cells in each square millimeter was then calculated from the unit area counts. The proportion of surviving cells was determined by dividing the number of cells in each experimental animal by the mean of the control group. The mean proportions of surviving cells for each age group are graphed in Fig. 10–21. Regression analysis (SAS, regression procedure) was used to analyze cell packing density differences between the control and x-irradiated groups. The results indicated three different patterns of change, one in the ventricular zone, another in the subventricular and intermediate zones, and a third in the cortical plate.

10.5.2 The Ventricular Zone

In the ventricular zone (*upper left graph,* Fig. 10–21), x-irradiation destroys only about half of the cell pop-

[1] The section chosen for analysis was at the level where the olfactory bulb (visible from E16 on) extends farthest anteriorly, or at an intermediate mediolateral level between E13 and E15. A strip of dorsal neocortex halfway between the frontal and occipital poles was studied in detail.

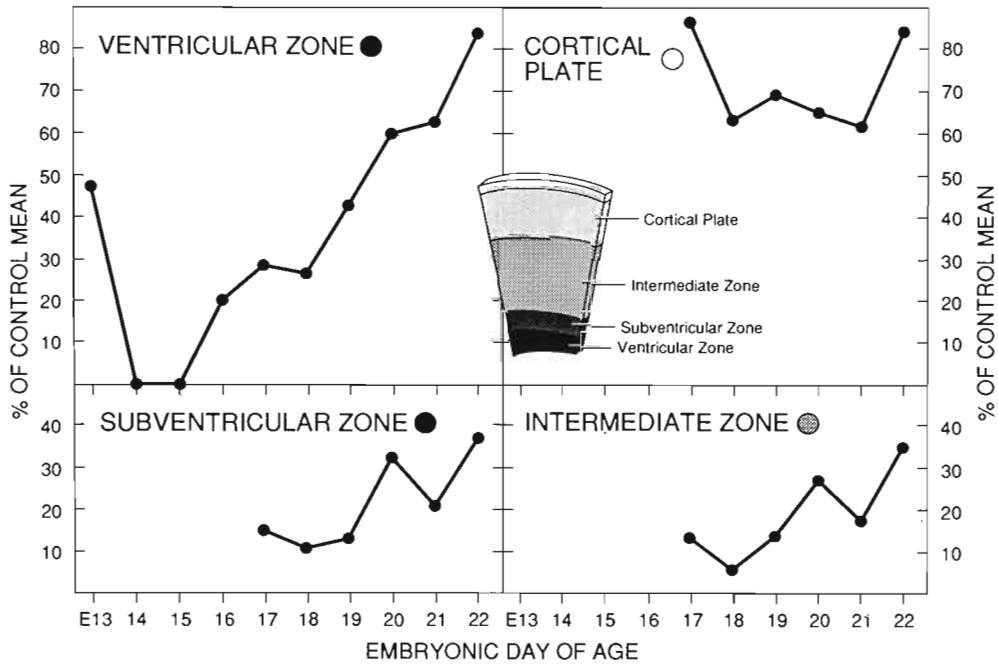

FIG. 10–21. The proportions of cells surviving 6 hours after an exposure to 200 R x-rays. For each experimental animal, the proportion of surviving cells was equal to the number of cells divided by the mean number of cells in the control group times 100; averages for the experimental groups are shown in the graph. Note that pyknotic debris was not quantified, only intact and normal cells. In the ventricular zone (*upper left*) radioresistance increases during embryonic development. Cells are highly radiosensitive throughout development in the subventricular and intermediate zones (two bottom graphs), while a majority of the cortical plate cells are radioresistant (*upper right*).

the lateral cortical stream, they are older than the newly arriving neurons in the dorsal cortical plate that have spent one day or less migrating directly radially (Chapter 9). That age difference may account for the differential radiosensitivity of the dorsal versus lateral cortical neurons. The spared cells in the subventricular zone may be those that are migrating laterally.

10.5 CHANGING RADIOSENSITIVITY OF DIFFERENT CELLULAR COMPONENTS OF THE DEVELOPING CORTEX: A QUANTITATIVE ANALYSIS

10.5.1 Steps in Data Collection and Analysis

Differences in the number of normal cells between control and x-irradiated rats were analyzed in sagittal sections of the dorsomedial neocortex from E13 to E22.[1] The ventricular zone (neuroepithelium) was studied throughout the entire observation period. Since the subventricular zone, the intermediate zone, and the cortical plate are not distinct in the dorsal neocortex until E17, quantification in those layers began then. In both control and experimental animals all cells were counted using a 40× objective and a 10 × 10 ocular grid that delimited a total area of 0.333 mm^2 at a final magnification of 625×. In animals that had been exposed to x-ray, only surviving cells were counted. (The number of pyknotic fragments were not counted since there may be several of them for each killed cell.) The total number of cells in each square millimeter was then calculated from the unit area counts. The proportion of surviving cells was determined by dividing the number of cells in each experimental animal by the mean of the control group. The mean proportions of surviving cells for each age group are graphed in Fig. 10–21. Regression analysis (SAS, regression procedure) was used to analyze cell packing density differences between the control and x-irradiated groups. The results indicated three different patterns of change, one in the ventricular zone, another in the subventricular and intermediate zones, and a third in the cortical plate.

10.5.2 The Ventricular Zone

In the ventricular zone (*upper left graph,* Fig. 10–21), x-irradiation destroys only about half of the cell pop-

[1] The section chosen for analysis was at the level where the olfactory bulb (visible from E16 on) extends farthest anteriorly, or at an intermediate mediolateral level between E13 and E15. A strip of dorsal neocortex halfway between the frontal and occipital poles was studied in detail.

ulation on E13, as seen in the low-magnification photomicrographs in Fig. 10–2, and at higher magnification in Fig. 10–14B. There is total destruction of neuroepithelial cells on E14 and E15, as seen at low magnification in Figs. 10–3 and 10–4, and at higher magnification in Fig. 10–15B. From E16 to E22, the proportion of surviving cells increases in a nearly linear pattern, as shown at some selected ages at low magnification in Fig. 10–7, and at higher magnification in Fig. 10–18B. The increased sparing of neuroepithelial cells is associated with the transformation of the totally collapsing neuroepithelium to one that shows (at least in some regions) patchy collapse and eventually no collapse.

Regression analysis of the quantitative data established that the effectiveness of 200 R x-ray in killing neuroepithelial cells systematically diminishes over time (control slope = 0.048; x-ray slope = 0.309; F = 103.47; df = 1, 50; $P < 0.0001$). On E21, 38% of the cells are killed by the x-rays, a significant reduction below controls (F = 31.52, df = 1, $P < 0.0001$, F test). However by E22, only 17% of the cells are killed, and the x-irradiated group is not significantly different from the control group (F = 2.12; df = 1, 50; $P > 0.05$).

Very few neocortical neurons originate on E13, when the survival rate is at the 50% level. The extreme vulnerability of the neuroepithelium to 200 R x-ray between E14 and E18 coincides with the most active period of cortical neurogenesis. Neurogenesis first becomes prominent in the neocortex on E14, when most of the Cajal-Retzius cells in layer I originate and remains active in the dorsomedial neocortex until E18 (Chapter 3). During that time, the survival rate is either 0% (E14 and E15) or well below 50% (E16 to E18). By E21, [^{3}H]thymidine autoradiographic labeling characteristics in the ventricular zone suggest that it has changed into the primitive ependyma (Chapter 4), and a large proportion of the cells survive. Our interpretation of the continual increase in the survival rate of neuroepithelial cells from E16 onward is that, as fewer and fewer neurons are produced, the proportions of radiosensitive neuronal precursors decrease and radioresistant glial/ependymal precursors increase. Several years ago, we showed (Altman et al., 1968) that germinal cells giving rise to migratory cell populations, specifically neuronal precursors, are more radiosensitive than are germinal cells whose progeny do not migrate, such as ependymal precursors and some glial precursors.

10.5.3 The Subventricular and Intermediate Zones

In contrast to the more mature lateral cortex, x-ray exposure induces a great amount of cell death in the dorsomedial subventricular and intermediate zones (compare iz in Figs. 10–19A and B). The quantitative data suggest that, throughout embryonic development, the dorsomedial subventricular, and intermediate zones contain predominantly primitive cells that are highly radiosensitive.

In the subventricular zone (*lower left graph,* Fig. 10–21), 85–90% of the cells are killed between E17 and E19, and 60% are still killed on E22. When data between the control and experimental groups were contrasted with an F test on E17, E20, and E22, the experimental group was always significantly below controls (E17: F = 156.01; df = 1, 50; $P < 0.0001$; E20: F = 229.2; df = 1, 50; $P < 0.0001$; E22: F = 37.83; df = 1, 50; $P < 0.0001$). However, statistical analysis of the regression lines for the control group and the experimental group indicated significantly different slopes (control = 0.002918; experimental = 0.262036; F = 18.3; df = 1; $P < 0.0001$), indicating that x-irradiation was less effective in killing cells as development progresses.

In the intermediate zone (*lower right graph,* Fig. 10–21), 95% of the cells are killed on E18, and 65% are still killed on E22. Contrasts of the data for E17, E20, and E22 indicated that the experimental group was always significantly below the control group (E17: F = 137.2, df = 1, $P < 0.0001$; E20: F = 200.53, df = 1, $P < 0.0001$; E22: F = 32.41, df = 1, $P < 0.0001$). However, the regression lines of the control data (slope = −0.275175) and the experimental data (slope = 0.017866) were significantly different (F = 16.26, df = 1, $P = 0.0002$), indicating that the destruction produced by x-ray decreased with increasing age.

Evidently, the subventricular and intermediate zones are composed of a higher proportion of radiosensitive cells than the neuroepithelium at corresponding ages (compare data in Fig. 10–21). Our [^{3}H]thymidine autoradiographic studies indicate that the majority of cells in these zones are young neurons that are either sojourning in specific bands (Chapter 7) or are migrating to the cortical plate (Chapter 9). The x-irradiation data presented here show that these neurons are highly radiosensitive while they are in the dorsomedial cortex.

Developmental anatomical studies indicate that axonogenesis begins while young neurons are in the intermediate zone (Wise et al., 1977; Schreyer and Jones, 1982; Cabana and Martin, 1985, 1986; Schwartz and Goldman-Rakic, 1986). Although the onset of cell differentiation is usually associated with an increase in radioresistance, axonogenesis apparently does not offer protection for young cortical neurons in dorsomedial areas because they are killed in large numbers.

10.5.4 The Cortical Plate

In contrast to the great radiosensitivity of cells in the subventricular and intermediate zones, a high propor-

tion of cells are spared in the cortical plate (*upper right graph,* Fig. 10–21). Although there is a dip in the survival curve so that fewer neurons are killed on E17 (17%) and E22 (15%) than between E18 and E21 (30–40%), the regression lines of the data from the control and experimental groups had the same slope (intercept = −0.13), indicating that the x-ray effect is constant during the observed period of time. We compared control and x-ray data with an F test at three ages: E17, E20, and E22 and found that x-irradiation remains effective in reducing the number of cells in the experimental animals below control levels (E17: $F = 16.44$; $df = 1, 50$; $P < 0.0001$; E20: $F = 52.60$; $df = 1, 50$; $P < 0.0001$; E22: $F = 18.59$; $df = 1, 50$; $P < 0.0001$). Our interpretation is that the radioresistant majority (60–80%) of cortical plate cells are the settled neurons, while the radiosensitive minority (20–40%) are the primitive neurons migrating to their settling sites in the superficial cortical plate. The higher survival rate on E17 may be related to the finding that the first cortical plate cells are early differentiating subplate neurons (Chapter 5). Since few permanent-resident, immature neocortical neurons have reached the dorsomedial cortical plate on E17, the more mature subplate neurons constitute most of the cortical plate, and fewer of these are killed by x-irradiation. The dip in the survival rate from E18 to E21 may be caused by incoming waves of immature neurons that are still radiosensitive. Since neuronal migration into the dorsal cortical plate declines by E22, the overall survival rate increases.

10.6 POSSIBLE LONG-TERM EFFECTS OF HAZARDOUS INFLUENCES ON CORTICAL DEVELOPMENT[2]

Although our focus in this chapter is on the effects of x-irradiation, any trauma or environmental hazard that reduces the number of cortical neurons might have comparable consequences. Experimental results in the hippocampus (Bayer and Altman, 1975a, 1975b) and the cerebellum (reviewed in Altman, 1982) indicate that there is no compensatory regeneration following trauma during the period of neurogenesis and/or cell migration that produces depletion of cell number. For example, if one exposes the hippocampus to 200 R x-ray on P2 and P3, the period when dentate granule cell neurogenesis is at its peak, there is a 60% reduction in cell number on P30, and that remains constant up to the fourth postnatal month (Bayer and Altman, 1975a). The deficit appears in spite of the fact that dentate granule cells continue to originate long after P3 (Bayer and Altman, 1974; Bayer, 1980a); in fact, dentate granule cell neurogenesis persists at a low level into adulthood (Bayer, 1982; Bayer et al., 1982). Evidently, the surviving precursor cell pool of the dentate granule cells lacks a feedback mechanism that would either increase the rate of cell proliferation or prolong the period of proliferation to compensate for a reduction. Similarly, there is no evidence of compensatory neurogenesis after x-irradiation of the postnatally forming granule cells in the cerebellum (Altman, 1982) and olfactory bulb (Bayer and Altman, 1975b). Our general conclusion is that neuronal populations do not have a compensatory regenerative capacity and any insult that produces reduction in the numbers of neurons has a permanent effect.

The consequences of killing neuronal precursors or young neurons during development goes far beyond a simple quantitative reduction in cell number. Substantial loss in a neuronal population can distort the morphogenesis of other neurons that depend upon the decimated population for cues to structural modification (Ostertag, 1956). For instance, if the proliferative cells of the cerebellar external germinal layer are decimated soon after birth, the morphological organization of the cerebellar cortex is profoundly affected (reviewed in Altman, 1982). The normal foliation pattern of the cerebellar cortex is distorted, the alignment of Purkinje cells is jumbled, and the Purkinje cells fail to develop their characteristic dendritic arborization. The behavioral consequences are also severe and these animals display locomotor and postural abnormalities that resemble the effects of extirpation of the entire cerebellum (Altman, 1975b). Even when x-irradiation is begun late during development and there are no gross abnormalities in cerebellar morphology, there are still profound behavioral consequences. The reduction of the granule cell population of the hippocampal dentate gyrus also produces behavioral consequences comparable to removal of the entire hippocampus (reviewed in Altman, 1986, 1987).

There are only a few studies currently available about the enduring consequences of cell reduction in the cerebral cortex. A single exposure to low-level x-irradiation on a specific day produces a cerebral cortex that is lacking a corpus callosum (Jensen and Altman, 1982) and results in abnormal cortical lamination (Ferrer et al., 1984; Jensen and Killackey, 1984). There are several reports about the adverse behavioral consequences of x-irradiation (in the dose range of 100–300 R) in E13 to E18 rats on locomotion, maze learning, passive and active avoidance learning, and sensory discrimination during adulthood (reviewed in Furchtgott, 1975; Hicks and D'Amato, 1978). A difficulty with these behavioral studies is that irradiation *in utero* affects many brain structures in addition to the cerebral cortex.

An even more difficult task is to relate the experi-

[2] We are grateful for the advice and assistance of Jans Muller, M.D., Department of Pathology, Indiana University School of Medicine, in the writing of this section.

mental findings in rats and other laboratory animals to the many abnormalities of cortical development in man. In the laboratory setting, both the characteristics of the insult and its time of application are known, whereas neither of these are known in the clinical setting. Among teratologists, there is a distinction between primary malformations, which result from a faulty blueprint ("Bauplan"), as opposed to secondary malformations that are the result of destruction by environmental agents. These distinctions go back to Schwalbe (1906). Because the central nervous system has a very long developmental sequence, beginning from the earliest stage of embryogenesis and continuing after birth, it is the most common site of congenital malformations when compared to other organ systems (Ludwin and Norman, 1985). In the full-term infant, the most common site of dysplasia is the cerebral cortex (Menkes, 1985). The physiological and behavioral consequences of cortical dysplasias range from the dyskinesias of cerebral palsy (those attributable to upper motor neuron rather than extrapyramidal abnormalities) to mental retardation (Benda, 1952; Cruickshank, 1976).

A frequently reported and severe cortical dysplasia is holoprosencephaly, the failure of cleavage of the prosencephalon (DeMeyer, 1977). This defect is often associated with the absence of nasal cavities, olfactory aplasia, or arhinencephaly, and the development of a single eye (cyclopia). Since family clustering of cases has occurred more often than chance, holoprosencephaly may be caused by a genetic defect, but it can also be produced by experimental teratogenetic agents, such as the alkaloid cyclopamine (DeMeyer, 1977). Whatever the cause, the defect is manifest during the early phase of embryonic development when the single prosencephalon is being transformed into a two-chambered telencephalon and a diencephalon (Chapter 2).

Once the telencephalic vesicles have formed, three other cortical dysplasias become manifest that result in abnormal folding of the cerebral cortex (Bresler, 1899). Lissencephaly, the absence of gyri, and pachygyria, a reduced number of gyri, are characterized by a rather disorganized layering in the cortical plate. There are transitions to polymicrogyria, characterized by an increased number of very shallow gyri where the existing cortex has only three layers. All of these dysplasias are associated with a greatly depleted number of neurons, most severe in lissencephaly and least severe in polymicrogyria (Schob, 1930; Larroche, 1984). The abnormal folding results from an altered ratio between afferent fibers and intrinsic cortical cells. In some cases there is good evidence that the periventricular germinal matrix is diseased, as in cytomegalovirus ventriculitis. In other cases where the periventricular germinal matrix is not obviously diseased, the general cause is ascribed to a failure of cell migration. However, that could also mean a severely reduced number of neurons that will migrate.

Another developmental disorder of the cortex lies in the abnormal location of neurons referred to as *heterotopias*. Heterotopias may occur at three different sites. (1) In nodular heterotopias, clusters of gray matter may be found near the ventricle. This could possibly result from the regenerative process subsequent to rosette formation after patchy neuroepithelial collapse, as described by Hicks and D'Amato (1966). That type of heterotopia is a secondary effect of interference with the normal timetable of neurogenesis. (2) There are heterotopias in the deep white matter, sometimes composed of only single cells. Jensen and Killackey (1984) have produced heterotopias of layer V in the white matter with x-irradiation. (3) In laminar heterotopia, the layers of the cerebral cortex are in disarray (Friede, 1989). Laminar heterotopias have been experimentally induced in the cerebellar cortex with x-irradiation (reviewed in Altman, 1982).

In view of the late formation of the corpus callosum (Chapter 2), it is often abnormal, either secondary to earlier abnormalities or as the primary site of malformation. There are two examples of the former condition. (1) In holoprosencephaly, the corpus callosum is not found in a compact fiber bundle because the two separate cerebral hemispheres have not formed; instead, the callosal fibers are intermingled with the association fibers. (2) In lissencephaly, pachygyria, and polymicrogyria, the corpus callosum is always severely reduced because many of the neurons that contribute callosal fibers are not there. There is a true malformation, *agenesis of the corpus callosum,* where the callosum itself is directly affected. This defect is probably brought about by abnormalities expressed late in development or by late environmental insults. Whenever agenesis of the corpus callosum occurs, the fibers that would normally cross the midline run parallel to it in large fiber tracts, as described by Probst (see Silver and Ogawa, 1983). Agenesis of the corpus callosum can be induced by x-irradiation on E17 in rats (Jensen and Altman, 1982). Silver et al. (1982) induced agenesis of the corpus callosum in normal mice by lesioning the glial sling that crosses the midline 2 days before callosal axons decussate. In genetically acallosal mice, the implantation of a glia-coated cellulose bridge can induce the callosal fibers to cross the midline (Silver and Ogawa, 1983). A severe reduction to total loss of the corpus callosum can also be induced by exposing pregnant mice to x-irradiation on gestation day 14.5, which retards the initial appearance of the glial sling and the subsequent death of the cells that compose it (Schneider and Silver, 1990).